Open Ceramics 16 (2023) 100483

Contents lists available at ScienceDirect

Open Ceramics

journal homepage: www.sciencedirect.com/journal/open-ceramics

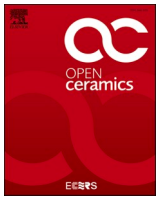

Review: Tailored microstructures in the system tricalcium phosphate-wollastonite-diopside for bone regeneration scaffolds

Carmen Baudín *, Pilar Pena

Instituto de Cerámica y Vidrio, CSIC, Kelsen 5, 28049, Madrid, Spain

ARTICLE INFO

Handling Editor: Dr P Colombo

Keywords:
Bioceramics
Bone regeneration
Scaffolds
Mechanical behavior
Tricalcium phosphate
Wollastonite
Diopside

ABSTRACT

Tissue engineering constructs (TECs) combining resorbable scaffolds, cells and/or reactive agents are required for bone regeneration. New green ceramic processing methods allow fabricating layered and gradient porous structures. Dense bioceramics with sufficient strength that keep their microstructure when incorporating porosity are required. Bioceramics in the system tricalcium phosphate-wollastonite-diopside are reviewed. Tailoring of microstructures to improve their mechanical and biological behaviors and their potential for TECs are analyzed. First, a brief discussion on bone properties and requirements for biomaterials and the capabilities and limits of glasses and glass-ceramics formulated in the system is done. Then, the relationships between the microstructure and the mechanical behavior of single-phase and composite bioceramics are discussed. TCP-D-W microstructures with adequate mechanical performance support viability and osteogenic differentiation of human mesenchymal stem cells (hASCs) and their colonization by hASCs presents specific morphological features that make them adequate for TECs.

1. Introduction

Bone-associated diseases due to aging, traumas, congenital defects or surgical removal of tumors are one of the most important current public health problems. Bone tissue possesses a natural regenerative capacity that is sufficient for the healing of small sites of damage, such as some types of fractures, however, defects that exceed a critical size (typically >2 cm, depending on the anatomical site) cannot heal unaided. Specific clinical intervention for functional restoration and complete healing is usually needed for large defects.

As a result, bone is the second most commonly transplanted tissue worldwide, with millions of operations using bone grafts and bone substitute materials annually [1,2]. Frequently, treatments involve implantation of a temporary or a permanent prosthesis, which is challenging, especially when dealing with large defects.

In most cases, bone grafts harvested from the patients themselves (autografts) are used. Also, animal derived (xenografts) and human allografts are suitable solutions. However, all biological-type transplants have drawbacks due to limited amount of donor tissues, donor site morbidity, and/or potential risks of immunological incompatibility and disease transfer.

Synthetic biomaterials might avoid the immunological and disease risks. In addition, they can be produced in large quantities with acceptable costs and are relatively easily certified for clinical applications [3]. Thus, they present advantages for the healthcare systems which are overcharged by the increase of bone diseases related to ageing and accidents. Even though synthetic biomaterials are widely used for repair, regeneration, and replacement of damaged bone, their performance is still considered inferior to that of autologous bone so they deserve further improvements before they could successfully replace treatments based of natural bone grafts and biologics. Therefore, one of the main subjects of materials science is the research on artificial materials for bone tissue therapies.

Granules of bioactive and resorbable materials are successfully used for bone repair. However, their use is limited when dealing with large defects and/or load bearing applications. In such cases, it has been proposed the use of engineered structures combining resorbable scaffolds, cells and/or reactive agents as growth factors or antibiotics: tissue engineering constructs (TEC). In the ideal case, these structures would facilitate host cells to deposit extracellular matrix (ECM) and replace the scaffold structure over time.

Apart from an adequate design of the scaffold architecture, the properties of the material that constitutes the wall of the scaffold are basic for scaffold performance. Materials for scaffolds with a successful

* Corresponding author.
E-mail address: cbaudin@icv.csic.es (C. Baudín).

https://doi.org/10.1016/j.oceram.2023.100483
Received 28 July 2023; Received in revised form 2 October 2023; Accepted 2 October 2023
Available online 17 October 2023

balance between the properties needed for adequate cellular function and viability and adequate mechanical strength constitute a main research field. In this sense, the problem can potentially be solved by developing multiphase materials containing highly dissolvable phases and low resorbing phases with improved mechanical behavior. As it will be discussed in this paper, the mechanical behavior of bio-glasses, glass-ceramics and ceramics (in general bioceramics) for bone regeneration is a recurring issue.

The classical thinking about scaffolds for bone regeneration envisages monolithic scaffolds with sufficient structural integrity while containing high amounts of large connected pores. Such an approach can be replaced nowadays thanks to the available new green ceramic processing methodologies that permit the fabrication of layered and gradient structures with different levels of porosity. Then, solving the problem of mechanical performance of bioceramics can be approached by the development of relatively dense materials with sufficient strength that keep their microstructure when they incorporate porosity. In this way, the mechanical performance of the wall of the porous structure is assured. This approach requires the selection of compositions and sintering processes that lead consistently to similar phase content and distribution starting from green bodies with different characteristics.

In the field of ceramics, the most successful polycrystalline bioceramics for bone regeneration are calcium orthophosphates ($CaPO_4$-based, CPs), in particular, hydroxyapatite ($Ca_{10}(PO_4)_6(OH)_2$; HAp) [4,5], β-tricalcium phosphate (β-$Ca_3(PO_4)_2$; β-TCP) [4,6], and their mixtures called biphasic calcium phosphates (BCP) [7–9] Their interest is based on the compositional similarity with the main component of bone, an apatitic calcium phosphate, which assures their biocompatibility and simplifies the regulatory path leading to the approval for clinical use. Some CPs, with specific properties, are claimed to possess the bone regenerative potential *in vivo* comparable to that of autologous bone. Main drawback of these materials is that they usually lack osteoinductive potential and their poor mechanical performance.

The development of CPs-based ceramics and ceramic-ceramic composites incorporating biologically active ions for inorganic scaffolds with sufficient mechanical properties and adequate biological response

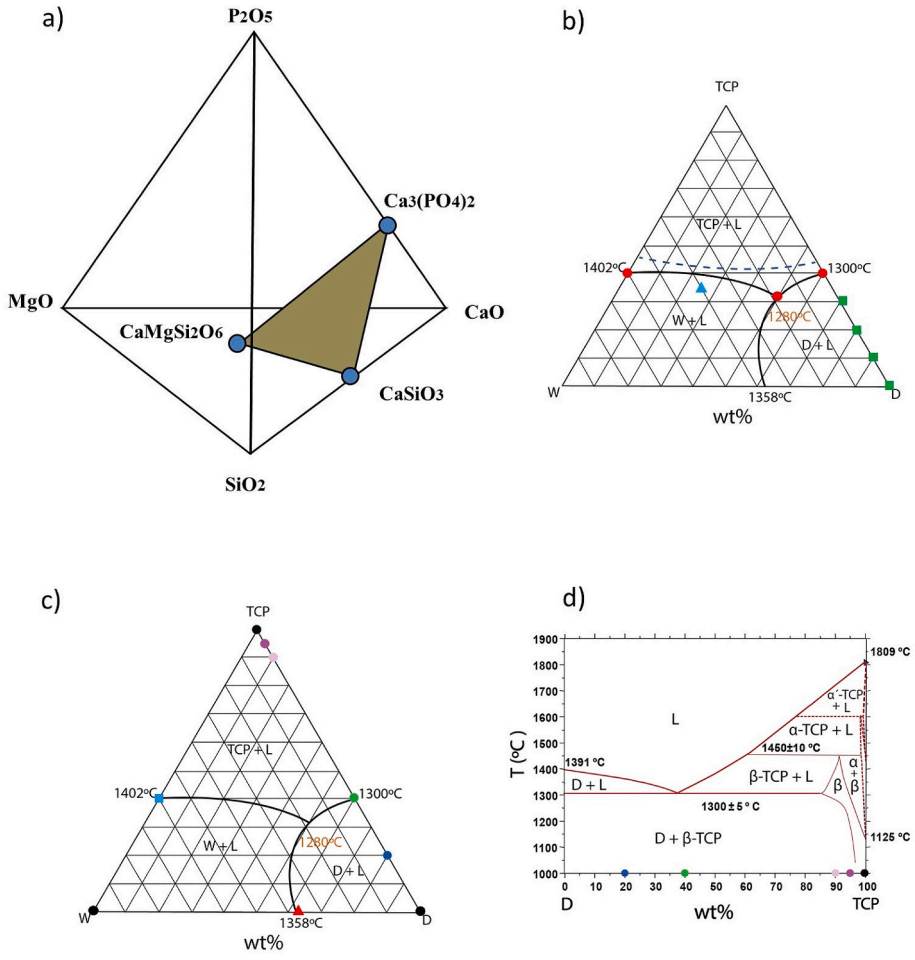

Fig. 1. a) Schematic representation of the Quaternary phase equilibrium diagram showing the location of the $Ca_3(PO_4)_2$–$CaSiO_3$–$CaMg(SiO_3)_2$ system.
b)-c) Liquidus surface of the system TCP-W-D according to Magallanes-Perdomo et al., 2012 [10]
b) Bio-glass and glass-ceramic compositions studied by different authors are plotted.
Red circles: Magallanes-Perdomo et al. (40TCP-60W; 40TCP-60D and 31TCP-19W-50D. [10,61,62]; Blue triangle: Kokubo et al. (36TCP-40W-24D). [10,59]; Green squares: Kapoor et al. [57,58]
c) The compositions of the polycrystalline bioceramics studied by different authors are plotted.
Black circles at the vertices of the triangle: single-phase materials, different authors (discussed in the text); Blue square: Bioeutectic® (60W-40TCP) de Aza et al. [101];
Red triangle: eutectic composition of the W-D system (37W-63D) Sainz et al. [114];
Circles along the TCP-D: different compositions developed by our group (discussed in the text).
d) Pseudo-ternary system TCP-D [112,113]
Circles of different colours show the compositions of the polycrystalline bioceramics studied by our group. The color code is the same as in Fig. 1 c).

Table 1
Mechanical properties of human bones, bio-glasses and glass-ceramics.
Bones are tested with the cortical bone oriented in the maximum length. Toughness of bones is determined by SEVNB.
Toughness of glasses and glass-ceramics are determined by indentation.

Material	First author and reference	Strength (MPa)			Young's modulus (GPa)				Fracture toughness K_{IC} ($MPam^{1/2}$)
		Uniaxial Compression	Bending	Uniaxial Tension	Dynamic	Bending	Uniaxial Compression	Uniaxial Tension	
Human bone									
Cancellous *femur **vertebrae	Currey [15]	2-4* 0.7–7**	–	–			0.2–0.3*		
Cortical femur		180–240	160–180	90–100		16	20	12	6.4 5.1
Tibia	Dapaah [17]								2.4–5.3
Skull composite	McElhaney [16]			43 ± 18					
	Clifford Lee [12]		42 ± 14 53 ± 13			4–18			
Skull cortical	McElhaney [16]			79 ± 26					
Glasses									
Bioglass^R (45S5)	Peitl [55]		60 ± 10	42		60			0.6
Ap mother glass	Kokubo [59]		70						0.8
TCP-W	Magallanes-Perdomo		102 ± 9		83 ± 5				0.8 ± 0.1
TCP-D	[10]		105 ± 6		94 ± 1				0.7 ± 0.1
TCP-W-D			105 ± 15		92 ± 2				0.8 ± 0.1
Glass-ceramics									
Ap-W Cerabone	Kokubo [59]	1080	220			118			2.0
62D—38TCP	Ashizuka [67]		220 ± 7		126 ± 1				2.4 ± 0.1

is a research field of increasing interest. In particular, huge efforts have been dedicated to the development of materials containing β-TCP with compositions in the quaternary system $CaO–P_2O_5–SiO_2–MgO$, in particular, in the ternary system $Ca_3(PO_4)_2–CaSiO_3–CaMg(SiO_3)_2$ (tricalcium phosphate, TCP, - wollastonite, W, -diopside, D) with improved bioactivity and mechanical behavior. The compositions of the materials are summarized in Fig. 1. Fig. 1a) shows the location of the ternary system TCP-W-D in the quaternary system $CaO–P_2O_5–SiO_2–MgO$. The liquidus surface of the ternary system, according to Magallanes-Perdomo et al., 2012 [10], is plotted in Fig. 1b)-c), with the compositions of the bio-glasses, bio-glass-ceramics and polycrystalline bioceramics located in it. This system has a eutectic point at relatively low temperature, 1280 °C and a large compositional glass forming zone (Fig. 1b)).

In this work, the development of polycrystalline bioceramics in the system TCP-W-D is addressed. The tailoring of the microstructures to improve their mechanical and biological behaviors and their potential to constitute walls of scaffolds for bone regeneration is analyzed. After a brief discussion on bone properties and the requirements of biomaterials for bone substitution and repair, capabilities and limits of glasses and glass-ceramics formulated in the system are described. Then, single phase and composite polycrystalline materials are discussed focusing the relationships between the microstructure and the mechanical behavior. Last, our main results on the biological behavior of optimized microstructures seeded with human mesenchymal stem cells (hASCs) are summarized.

It is to note that different testing methods and specimen sizes and preparation (e.g: surface treatment) are used to characterize the mechanical behavior of materials in different works, which hinders the comparison between the actual figures. In this review, an effort has been done to carefully consider the testing methods in order to make meaningful comparatives. Strength data from different materials obtained using the same testing method and similar specimen sizes are considered. Bending strength data are compared only between those of specimens with similar surface treatments. Tensile strengths from diametral compression of discs test (DCDT) [11] are used when possible. This method is preferred because failure of DCDT specimens starts from the central plane of the disc specimens so results are not determined by the surface status of the specimen and the volume of material that is characterized is bigger than in bending tests. Weibull distributions of the tensile strength values for nominally identical specimens are analyzed. The Weibull modulus, m, which modulates the shape of the distribution is a measure of the reliability of the material while the characteristic strength, σ_0 is the strength with a 63 % probability of failure. Results for specimens of different sizes are corrected using the Weibull statistical approach before comparison.

2. Mechanical behavior of bones

Bone is a complex hierarchical structure. At the lower levels of hierarchy, bone is a composite of collagen and nanoparticles made of collagen and hydroxyapatite [12–14]. Its microstructure/texture presents different scales: the nanosized twisted peptide chains, the hydroxyapatite-impregnated twisted collagen fibrils at the scale of tens of nanometers, collagen fibers with diameters around 1 μm, the lamellar structure of collagen fiber bundles, of several micrometers and the osteon structures, with sizes of several hundred micrometers.

Such structure is responsible for the specific mechanical behavior of bones that presents toughening mechanisms at different scales, i. e: short- and long-range toughening. In addition, bone structure is anisotropic, and constituted by a porous bulk, cancellous bone, surrounded by a cortical shell. Cortical bone has a density around 2 g/cm^3 and total porosity of about 6 %. Density of cancellous bone is between 0.2 and 0.8 g/cm^3 and porosity can reach 80 %. The mechanical behavior in the longitudinal direction of the cortical shell is different from that in the transverse orientation. Such mechanical behavior leads to the mechanical properties measured being dependent on specimen size and testing method.

In addition, bone presents the specific characteristics of a living material, which mechanical behavior is determined by histology, and properties are highly dependent on the specie and age of the individual from who specimens are obtained. Consequently, the range of reported mechanical properties of bones is broad. This subject was deeply analyzed by Currey in a comprehensive paper [15]. As highlighted by Currey, it is important to control the environment of the specimens before and during testing in order to avoid dehydration of the specimens.

Bones with different function differ strongly in shape and structure.

Long bones, such as the femur or the tibia, provide stability against bending and buckling. Short bones, such as the vertebra or the vertebra or the head of the femur, support mainly compressive stresses. Plate-like bones, such as the skull, protect and maintain the shape of vital organs. The shape and size of the different bones also determine the testing possibilities.

In order to have a term of comparison between the mechanical properties of the considered bioceramics and bones, some properties extracted from Refs. [12,15–17] are summarized in Table 1. As mechanical tests are usually performed with specimens oriented along the maximum length of the bone, results for such orientation are collected in the table.

Values of static Young's modulus and strength of human long bones (men) collected by Currey [15] show a dependence on the testing method (tension, compression, flexure), on the orientation of the specimen with respect to the applied load and on the degree of calcification. Most tests are done on whole bones and specimens extracted from the cortical part; cancellous (or trabecular) bone specimens are more difficult of extracting and testing. Maximum values of Young's modulus are obtained when the collagen fibrils are loaded longitudinally. In this case, values of about 20, 16 and 12 GPa correspond to femur cortical bone in uniaxial compression, bending and uniaxial tension, respectively (Table 1).

In general, reported values of Young's modulus of bioceramics are measured by ultrasonic methods. In order to compare to the static values of Young's modulus of bones, it has to be considered that, for the same material, flexure Young's modulus is about 20 % lower than that determined by ultrasonic methods. The reason is that these methods involve small and practically instantaneous deformations, so results are determined by the stiffest constituents of the materials.

Tensile strength values for femur collected by Currey [15] (90–100 MPa) are lower than bending and compressive strengths, as expected due to different specimen volumes subjected to the highest tractions. Compressive strengths are the highest, the high variability found in compression is attributed to the difficulty of machining specimens with parallel surfaces. It is important to have in mind that bones in bending do not behave elastically until fracture but the zone of the specimen in tension deforms plastically. Thus, the failure stress calculated as the modulus of rupture, i. e: assuming elastic behavior, is over-evaluated.

Strength values for cancellous bone reported by Currey [15] are much lower than those for cortical. There is a wide range of values of compressive strengths of cancellous specimens from lumbar vertebrae, between 0.7 a 7 MPa, decreasing with age. For femur cancellous bone, compressive strength of 4 MPa decreases to 2 MPa when age is over 71 years. As occurs with strength, reported compressive Young's modulus for femoral cancellous bone (≈0.2–0.3 GPa) are much lower than those for cortical bone.

Skull bones in the human (Fig. 2) are constituted by a well-defined shell of compact bone separated by a core of spongy cancellous bone called diploe. Reported values of strength are also summarized in Table 1. The high values of the standard deviations of strength are due to the naturally occurring variations of the diploe thickness and density. Tensile strength values around 40 MPa for the whole bone structure and 70 MPa for the compact part have been reported [12,16]. The slightly higher bending strength values found for the whole structure, between 45 and 50 MPa, as compared to tensile strengths, can be explained by the lower effective volume of bending specimens as compared to tensile ones. Skull bone repairing would require relatively thin TECs with specific shapes suitable for the individual and the particular defect. In addition, the mechanical solicitations that do not include bending or buckling are less severe than for long bones. Therefore, skull bone repairing appears as an opportunity for bioceramics.

Most measurements of toughness of bones consist on single-value characterizations of the property of cortical bone using SEVNB (single edge V notched beam) or double torsion tests. Some values for human tibia and femur [17] are included in Table 1 to be compared to the few

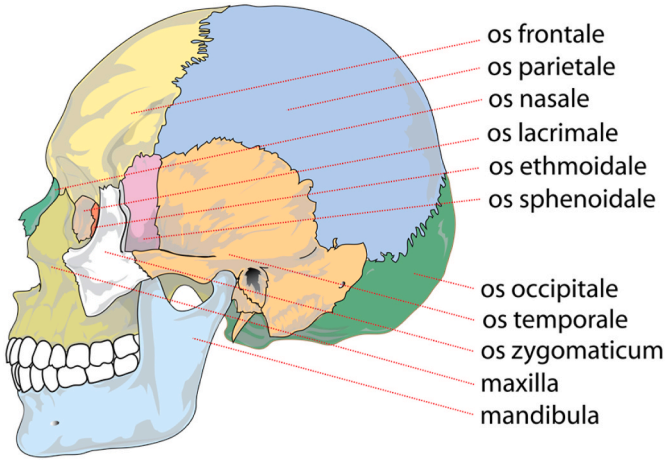

Fig. 2. Human adult skull showing the different bones.
Wikimedia commons
Mariana Ruiz Villarreal 2007.

reported toughness data for the bioceramics considered here. Specific analyses of toughening mechanisms and the associated properties can be found elsewhere [13,17]. As for strength testing, most measurements have been done with specimens of cortical bone oriented along the maximum length. Toughness in the most clinically relevant transverse orientation is the highest.

3. Biomaterials for bone substitution and repair

Almost inert materials, such as alumina or zirconia in the case of ceramics, are used for replacement of relatively large bones with load bearing responsibility such as in hips or teeth [18]. This first generation of biomaterials was initially developed during the 1960s and 1970s. The main goals searched for their development are to achieve a suitable combination of physical properties to match those of the replaced tissue and to reduce to a minimum the biological response to the foreign body once implanted [19].

Nearly-inert implants in the body are commonly surrounded by thin, acellular fibrous capsules due to the body's inflammatory response to foreign objects. Such interfaces between tissues and bioinert biomaterials present minimal adhesion between the implant and its host tissue, leading to interfacial movement. The need to correct this lack of adhesion was the objective of the initial development of bioactive materials that could bond to bone. By the mid 80′s, the "second-generation biomaterials", the bioactive materials, capable of originating a controlled action and reaction in the physiological environment were introduced [19]. Since then, different bioactive synthetic materials have been proposed and used for bone repair and regeneration, including metals, polymers, and ceramics. An updated (2016–2022) summary of the different categories of bone graft materials and their biomedical potential is found in Refs. [1,20,21].

The standard concept of bioactive glasses, glass-ceramics and ceramics was initially identified by Hench et al. [22,23] in the early 1970's: "*A bioactive material is one that elicits a specific biological response at the interface of the material, which results in the formation of a bond between the tissues and the material*". The main historical facts of the initial period of bioactive glasses, glass-ceramics and ceramics (1969–1986) were described by Hench et al. [23] in 1987. The complicate mechanism of bonding identified by Hench et al. was composed of 11 steps [24], the common characteristic being the time-dependent formation of a biologically active hydroxycarbonate apatite (HCA) layer as bonding interface with the bone upon implantation. The basic facts related to the mechanisms of formation of this bond for materials with different compositions were summarized by

Hench [25] in 1991. The interfacial bonding occurs because the chemistry and crystalline structure of this HCA phase are similar to those of the mineral phase in bone. This kind of behavior was originally called type A bioactivity. Not all bioactive materials form the HCA layer. Hydroxyapatite bonds directly to bone and other materials such as tricalcium phosphate, diopside and wollastonite present different behaviors, as will be described later.

In the same category of second-generation biomaterials are included the resorbable materials. As described by Hench in 1980 [26] *"Resorption of biomaterials appears a perfect solution to the interfacial problem because the foreign material is ultimately replaced by regenerating tissues. Ideally, there is eventually no discernible difference between the implant site and the host tissue"*.

Further studies showed that the ionic products released from biomaterials stimulate osteoblast proliferation and differentiation *in vitro* [18]. Thus, the new concept of "third-generation biomaterials" in which bioactive materials should stimulate cell and tissue growth was proposed [19]. The initial goal of biomaterials replacing living tissues, such as bones, whose properties, in Hench's words [26] *"are a result of millions of years of evolutionary optimization and which have the capability of growth, regeneration and repair"*, has now been changed into the goal of regenerating the living tissues.

From the late 1970′s, glasses, glass-ceramics and ceramics have become increasingly used for bone repair and regeneration. This broad family of "bioceramics" presents the whole range of classically described implant-bone interactions [27]: nearly inert, porous for bone ingrowth and bioactive and resorbable. New materials are being developed searching improved capabilities for osteogenesis (bone regeneration) and angiogenesis (formation of blood vessels). Specially designed materials have been -and are being- developed, to support the demanding conditions of use that are especially harsh to ceramic materials: corrosive saline solutions at 37 °C under variable, multiaxial, cyclical mechanical loads [18]. Structural integrity of the materials has to be maintained during implantation and resorption, but also during manipulation *in vitro* before implantation (e.g: seeding).

4. Scaffolds for bone regeneration

As mentioned in the introduction, it has been proposed the use of engineered structures combining resorbable scaffolds, cells and/or reactive agents as growth factors or antibiotics: tissue engineering constructs (TEC) for repairing large effects and/or for load bearing applications. Comprehensive reviews on scaffolds for bone tissue engineering can be found in Refs. [1,2,28–31].

The rate of scaffold degradation should be synchronized with the rate of mineralized tissue deposition, for the gradual mechanical degradation of the scaffold to be compensated as it is replaced by regenerated bone tissue. In addition, the degradation products must also be biocompatible and must not interfere with the function of the bone-tissue- engineering system. For example, degradation must not substantially alter the local pH, which could impair scaffold mineralization.

The parameters of materials design for bone-tissue engineering should be established considering characteristics of the target bone tissue. As highlighted by Hutmacher et al. [30], it is *"by no means clear what defines an ideal scaffold"*. Since bones of human skeleton have very different dimensions, shapes and structures depending on their functions and locations, synthetic bone grafts of various sizes, shapes, porosity, mechanical strength, composition and resorbability would be necessary [28]. Moreover, it is needed to reach a compromise between incompatible required properties such as mechanical strength and high levels of interconnected porosity to allow colonization by cells, as described below [31].

Regarding structural integrity, scaffolds should provide sufficient initial mechanical strength and stiffness to substitute for the mechanical function of the damaged bone until it is regenerated and/or permit cell seeding of the scaffold *in vitro* without compromising scaffold architecture. However, the mechanical performance of synthetic materials is far from that of bones, which are living tissues that even have the capacity of changing their response depending on the specific solicitations. Keeping such a limit in mind, there is no agreement in the literature about the minimum target mechanical properties for bone scaffolds.

Ambitious goals would search for the ideal scaffold having properties comparable to those of cortical bone, as shown in Table 1: compressive strength 180–240 MPa, with a Young's modulus close to 20 GPa and a tensile strength of around 100 MPa. These mechanical properties would be complemented by porosity between 60 % and 90 % and an average pore size larger than 150 μm to allow cell colonization [2,6,32]. Still larger pore sizes and pore interconnections (≥100–300 μm) are needed to facilitate the infiltration of new blood vessels and perivascular nerve fibres, and the seeding of osteoprogenitor cells throughout the construct before implantation [1,30]

As signaled by Bohner et al. [33], *"a paradigm shift occurred at the turn of the millennium: instead of designing load-bearing bone graft substitutes, researchers aimed for bone graft substitutes providing a fast healing response, that is a fast turnover from a bone defect to mature (= mechanically competent) bone"*. In this sense, it has been proposed that a good balance between a high degree of porosity and mechanical properties comparable with cancellous bone should be sufficient for scaffold performance [27,34]. Composites of phases with different biological and mechanical responses are proposed for the scaffold to maintain such properties during its colonization by cells and resorption.

In addition, the specific function and shape of the bone to be repaired would determine the suitability of ceramic scaffolds. In this sense, ceramic scaffolds appear as adequate candidates for regeneration of the skull plate bones (Fig. 2), which have variable shapes and less strict mechanical requirements than long bones (Table 1), as discussed above. Layered and/or gradient structures can be envisaged to combine different levels of porosity.

5. Calcium orthophosphates

As described in the introduction, calcium orthophosphates ($CaPO_4$-based, CPs) are the most successful polycrystalline bioceramics for bone regeneration.

Calcium orthophosphates have been developed and used as bone repair materials for about one century. According to Dorozhkin [36], the first mentioned use of artificial calcium orthophosphates as healing materials goes back as far as the 1870's. However, the use of implantable biomaterials did not become practical until the generalization of aseptic surgical techniques. Therefore, calcium orthophosphates were considered for clinical application as fillers for bone defects in the 1920's [35] and incorporated in dentistry and orthopedics in the shape of granules or cements in the 1980's. Comprehensive reviews on calcium orthophosphates can be found in Refs. [4,28,32] while their historical development has been fully described by Dorozhkin [36].

CPs are biocompatible, bioactive and resorbable. As the solubility of CPs is pH dependent, their resorption is mostly controlled by their interaction with cells. Thus, concomitant material resorption and bone formation processes and the absence of biocompatibility issues due to the uncontrolled release of large amounts of degradation products are ensured [33,37,38]. In addition, this pH dependent behavior makes CaPs ideal encapsulating agents for drug and imaging agents because dissolution with release of the active agent would occur as pH decreases within the cell [37].

The extremely low toughness of CPs limits their application as sole constituents of scaffolds [4,37]. For hydroxyapatite (HAp), which is the CPs with the best mechanical behaviour, reported toughness values slightly vary with grain size and/or dopants and test technique (Table 3), being the maximum values of fracture toughness reported 1.1–1.2 MPa $m^{1/2}$ [39,40]. In addition, HAp presents the lowest bioactivity, so implants made of sintered HAp are found in bone defects for

many years after implantation [28].

Metals and polymers have been used to manufacture hybrid biomaterials trying to reach bone graft substitutes with high mechanical properties [28,32,33,41]. Polymer-CPs composites, polymeric coatings on the CPs parts and infiltration of the porous structures by polymers have been proposed to overcome the poor mechanical behaviour of CPs. In general, the incorporation of polymers implies the decrease of final porosity of the scaffold which might lead to the decrease of properties such as bioactivity or osteoconductivity and/or inadequate resorption behaviour. In addition, the structural integrity of the implant is lost once the quick dissolution of the polymer occurs and the release of large volumes of degradable polymers or metals might present biocompatibility problems.

6. The role of Si and Mg in bioceramics

One of the key parameters affecting all properties of ceramics is composition. Specifically, it determines the biological behavior of bioceramics. In this frame, increasing research interest is devoted to improve the capacity of CPs materials for desired biological effects (such as osteogenesis or angiogenesis) by the addition of biologically active ions [42,43]. Various bioceramics incorporating a wide range of bioactive ions – e. g: Mg^{2+}, SiO_4^{4-}, SiO_3^{2-}, Cu^{2+}, Sr^{2+}, Li^{+}, Ag^{+} – have been proposed aiming less expensive and potentially more robust alternatives to the inclusion of biomolecules such as growth factors.

Magnesium is the fourth most abundant trace element in the human body and the second most abundant cation within human cells after potassium. Approximately 60 % of whole-body magnesium is found in bones, where it contributes to form hydroxyapatite crystals [44].

Regarding silicon, considering that it is the third most abundant trace element in the human body, it seems more than plausible that it could have potential benefits to humans. However, such fact continues to be debated even though there are some reports on its beneficial role in bone mineralization and prevention of osteoporosis [44].

Laboratory tests using Ca–Mg–Si extracts from crystalline ceramics [45] and glasses [46,47] have demonstrated that the ionic products released during the dissolution of the biomaterial stimulate *in vitro* cell proliferation, osteogenic differentiation and angiogenesis as compared to tricalcium phosphate. Moreover, *in vivo* results using akermanite ($Ca_2MgSi_2O_7$) implants revealed that Si is a crucial element for the induction of angiogenesis during new bone formation, and for the acceleration of bone regeneration [48]. *In vitro* and/or *in vivo* cell proliferation and differentiation on different Mg^{2+} containing glasses, glass-ceramics and polycrystalline bioceramics have been reported (see Ref. [49] for review). It has been proposed that the improvement of the interactions of the bioceramics with osteoblasts is due to the modification of their surfaces by Mg^{2+} [50,51]. *In vitro* and *in vivo* experiments using akermanite ($Ca_2MgSi_2O_7$) and nagelschmidtite ($Ca_7Si_2P_2O_{16}$) as model Si and Mg-containing bioceramics found that the released ions significantly decreased the immune responses caused by macrophages as compared to a β-TCP reference material. It was suggested that the modification of the immune responses was due to the alteration of the ionic microenvironment between the implants and hosts [52].

As discussed in the introduction, several glasses, glass-ceramics and polycrystalline ceramics have been formulated in the ternary system tricalcium phosphate ($Ca_3(PO_4)_2$) – wollastonite ($CaSiO_3$) – diopside ($CaMg(SiO_3)_2$), (Fig. 1). In particular, huge efforts have been devoted to the study of polycrystalline bioceramics considering CPs doping with Mg^{2+} and/or SiO_4^{4-}, and the combination of different phases. In addition to benefits in the biological behavior, specific compositional changes and/combinations might improve the mechanical behavior as will be discussed in which follows.

7. Glass and glass-ceramics

The compositions of most existing bioactive glasses and glass-ceramics belong to the CaO– P_2O_5–SiO_2–MgO–Na_2O system and could contain small amounts of CaF_2, MgF_2, K_2O, and SrO [53,54]. Hydroxyapatite, wollastonite, β-TCP and diopside are the common precipitated crystalline phases in glass-ceramics. Different glass and glass-ceramics have been registered as commercial products (e.g: 45S5 Bioglass®, Cerabon®, Biosilicate® and CeravitalVR). Compositional innovation has broadened the application of glasses and glass-ceramics initially developed for bone regeneration, allowing their use for advanced biological properties such as nerve regeneration and cancer treatment [54].

Hench and co-workers first demonstrated bioactivity for a certain compositional range of glasses that contained SiO_2, Na_2O, CaO, and P_2O_5 in specific proportions. As differences with traditional soda–lime–silica glasses, the bioactive glasses present three main compositional features: SiO_2 amounts <60 mol%, high Na_2O and CaO contents, and high CaO/P_2O_5 ratios. Such features make their surface highly reactive when exposed to an aqueous medium, such as body fluids: when they become in contact with blood they undergo surface dissolution, releasing calcium, phosphate and soluble silica. Further studies showed that the Ca- and Si-containing ionic products released contribute to bioactivity, as both Ca and Si stimulate osteoblast proliferation and differentiation *in vitro* [18] leading to the concept of "third-generation biomaterials" described above.

Many bioactive SiO_2 glasses are based upon the formula of 45S5 Bioglass® (SiO_2: 46.1 mol% = 45 wt%; Na_2O: 24.4 mol%, CaO: 26.9 mol %; P_2O_5: 2.6 mol%), signifying 45 wt% SiO_2 (SiO_2 is the network former) and relatively low amounts of P_2O_5 (6 wt%). The compositions of these glasses are far from the typical compositions of soda lime glasses, which contain much more silica; the projection of the Bioglass® composition within the CaO–SiO_2–Na_2O system falls near a ternary eutectic point. Compositions and characteristics of these classical bioglasses can be found in Refs. [18,55] and the state of the art in terms of the use and commercialization of bioactive glasses was reviewed by Shearer et al. [56] in 2023.

Alkalis are useful for glass production because they decrease the temperatures of glass formation, however, alkali-containing glasses present some drawbacks such as high dissolution rate or low sintering potential. In addition, the considered glass compositions are generally unsuitable for the production of blocks or porous scaffolds because of the requirements of the thermal treatments necessary to reach sintered parts from green bodies. Sintering of glasses occurs by viscous flow, thus, the green bodies have to be treated at temperatures above their glass transition temperature and alkali-containing bioglasses crystallize immediately above their glass transition, losing their bioactivity.

Alkali-free bioglasses with high bioactivity, lower dissolution and good sintering behavior in comparison to alkali-containing bioglasses have been proposed and developed as alternatives.

The system CaO– P_2O_5–SiO_2–MgO–CaF_2 was used to develop a series of alkali-free bioactive glasses in which CaF_2 was the fluxing agent [57,58]. Compositions were located along the diopside–fluorapatite ($Ca_5(PO_4)_3F$)–tricalcium phosphate join. Glasses containing 10–20 wt% of TCP presented an optimum combination of properties to be used as biomaterials, not only in granular form but also for block implants or scaffolds.

These compositions exhibited high rate of bioactivity (i.e: development of HCA layer) *in vitro* and permitted adhesion and proliferation of MSCs as well as their osteogenic differentiation. In addition, as sintering preceded crystallization in glass compacts of the considered compositions, it can be hypothesized that the proposed compositions could be used to fabricate block implants and scaffolds.

A number of CaO–P_2O_5–SiO_2–MgO glass compositions were developed in the ternary system TCP-W-D, they are plotted in Fig. 1 b). The composition developed by Kokubo et al. [(36 wt % TCP, 40 wt % W, 24 wt % D] [10,59], is that of the mother glass of the Ap -W glass ceramic developed by these authors that will be discussed later. Magallanes-Perdomo et al. [10,61,62] proposed three eutectic bioglasses, two binary ones in the systems TCP-W (40 wt% TCP – 60 wt %

Table 2
Mechanical properties of a bioglass and various bioglass-ceramics with different compositions tested in air using the same specimen geometry and surface preparation by Kokubo et al. [64,66]. E: Dynamic; KIC: double torsión; γf: calculated.

	Glass fraction (wt.%)	Strength (3PB) (MPa)	Young's modulus (GPa)	Fracture toughness K_{IC} ($MPam^{1/2}$)	Surface fracture energy γ_f (J/m^2)
Glass (mother glass)	100	72 ± 25	89	0.8 ± 0.1	3.3
Glass-ceramic Ap	65	88 ± 12	104	1.2 ± 0.1	6.4
Glass-ceramic Ap-W	25	178 ± 20	119	2.0 ± 0.1	15.9
Glass-ceramic Ap-W-TCP	10	213 ± 17	124	2.6 ± 0.1	25.5

W) and TCP-D (40 wt% TCP- 60 wt% D) and one ternary TCP-W-D (32 wt% TCP-18 wt% W-50 wt% D) glass. Kapoor et al. [57,58], analyzed a series of TCP-D compositions with varying TCP/D ratios from 100 wt% D to 50 wt %TCP-50 wt %D. It can be observed that all the proposed glass compositions are located inside the glass formation area of the ternary system. Those developed by Kokubo et al. and Magallanes-Perdomo et al. have similar TCP amounts 30–40 wt%.

All eutectic compositions presented *in vitro* bioactivity, developing a biologically active HCA layer in SBF and capability for osteoblast adhesion and proliferation [60]. The TCP-D glasses proposed by Kapoor et al. [58] also developed a HCA layer in SBF while experiencing lower dissolution rates in Tris-HCl than 45S5 Bioglass®. In addition, *in vitro* studies in hMSC cultures showed that the compositions with 60 and 70 wt% diopside promoted cell adhesion and proliferation and cell differentiation into an osteoblastic phenotype. All the $CaO–P_2O_5–SiO_2–MgO$ glass compositions can be sintered at temperatures below the glass transition point so, as in the case of the glasses containing CaF_2, they could be proposed to fabricate blocks and scaffolds.

The excellent osteoconductive ability of glasses is widely exploited nowadays to stimulate bone regeneration. As described in the updated review (2023) by Shearer et al. [54], the morphology and delivery systems of bioactive glasses have evolved dramatically since the first devices based on 45S5 Bioglass®, from glass monoliths to granules and cements. At least 25 bioactive glass (BG) medical devices have been approved for clinical use by global regulatory agencies. Such materials are nowadays used in wide range of applications from monolithic implants and bone void fillers to cancer therapeutics. For specimens tested using similar testing methods and specimen preparation, Na_2O free and MgO containing glasses of binary (TCP-W, TCP-D) and ternary (TCP-W-D) compositions (Fig. 1 b) present values of Young's modulus and strength higher (30–40 %) than those of bioglass^R 45S5 and the mother glass developed by Kokubo and slightly higher toughness than bioglass^R 45S5 (Tables 1 and 2) [10,55,59]. The major disadvantage of bioglasses is their poor mechanical performance with average strength values similar to those of hydroxyapatite but even lower toughness (Tables 1–3), thus, lower reliability.

To reach improved mechanical behavior while maintaining the attractive biological properties, various bioactive glass-ceramics (GCs) have been developed from glass compositions in which precipitate different crystalline phases under heat treatment. Most frequently, the crystallinity of glass-ceramics varies between 30 % and 70 %. Their final phase compositions are constituted by combinations of metastable phases that depend on the range of temperature and time used for the processing. Therefore, as a family of materials glass-ceramics presents a broad range of properties.

Glass-ceramics using the above described $CaO–P_2O_5–SiO_2–MgO$ compositions plotted in Fig. 1 b) as mother glasses have been deeply analyzed by Magallanes-Perdomo et al. [10,61,62], Kapoor et al. [63] and Kokubo et al. [59,64]. The bioactivity of these glass-ceramics is of the same type as that of bioglasses, with their surface developing a biologically active hydroxycarbonate apatite (HCA) layer that bonds to bone. This apatite layer also develops *in vivo* at the interface between the biomaterial and bone, leading to the tightly bonding between the implant and bone. Apatite formation is nucleated by Si–OH groups on the surface, and is accelerated by calcium and silicate ions dissolved from the glass-ceramic.

The binary TCP-W glass exhibits internal crystal nucleation, whereas the binary glass TCP-D and ternary TCP-W-D glasses show surface

Table 3
Mechanical properties of dense polycrystalline single-phase bioceramics.

Material	First author and reference	Strength (MPa)		Young's modulus (GPa)	Fracture Toughness K_{IC} ($MPam^{1/2}$)
		Bending (3 PB)	Tensile DCDT	Dynamic	SENB/SEVNB
HAp	Liang [84]			120[a]	
	Nonami [40]	110		47	1.1
HP >99%T.D. d_{50} = 0.4 μm	Halouani [39]	137 ± 5			1.1–1.2
HP >99%T.D. d_{50} = 1.2 μm	Halouani [39]	100 ± 5			
HIP, transparentd_{50} = 1 μm	Boilet [85]	106 ± 11		122	0.92 ± 0.02
PsW synthetic	García-Páez [105]		σ_0 = 42 m = 3.5		
2M β-W 95 % TD SPS d < 1 μm	Long [102]	294 ± 11		46.5 ± 5.0[b]	2.0 ± 0.1
Diopside Dense	Nonami [40]	300		170	3.5

T.D.: theoretical density; HP: Hot pressing; HIP: Hot isostatic pressing; SPS: Spark Plasma Sintering.
σ_0 and m are the Weibull modulus and characteristic strength, respectively. σ_{av}: average strength.
[a] Calculated theoretical.
[b] No method described.

crystallization of diopside and or calcium apatite [10]. This later characteristic has to be considered when preparing glass-ceramic powders for sintering. The devitrification process of the TCP-W eutectic composition at ≈1000 °C produces monolithic micro-nanostructured glass--ceramics composed of a Ca-deficient apatite phase with wollastonite-2M (W-2M) homogeneously dispersed in an amorphous phase [61]. At 1375 °C, the material is composed of quasi-rounded colonies formed by a homogeneous mixture of pseudo-wollastonite and α-tricalcium phosphate (α-TCP) homogeneously dispersed in an amorphous phase [62]. Other microstructures, such as micro-nanostructured apatite–W-2M could be obtained by designing different thermal cycles [61]. In order to reach a similar micro-nano microstructure for D-containing compositions it is necessary to perform an intermediate milling step followed by subsequent sintering and devitrification.

Reviews on the fabrication method, properties and applications of biologically active glass-ceramics are found in Refs. [59,65].

Bioactive glass-ceramics present a wide range of strength and toughness values. As an example, values for different compositions tested using the same specimen geometry and surface preparation and the same testing methods [66] are summarized in Table 2. These materials were developed by Kokubo et al. (e. g: Refs. [34,59,66]) who were the first to develop bioactive glass-ceramics without Na_2O, in the mid 80′s in Japan. These authors had some failed attempts of producing glass-ceramics free of pores and cracks in the TCP-W-D system starting from a monolithic glass or even powdered glass. In order to overcome such difficulties, they added a small amount of CaF_2 (0.5 wt %) to the original composition (36 wt % TCP, 40 wt % W, 24 wt % D) and obtained crack free materials. The crystalline phases present were apatite, wollastonite and β-tricalcium phosphate, in proportions depending on the thermal treatment followed for crystallization. As observed in Table 2, a significant increase of toughness occurs as the amount of crystalline precipitated phases increases. The crystalline particles act as toughening sites leading to the increase in surface energy. Note that the highest toughness value corresponds to highly crystalline materials (10–25 wt% of glass). In the same way, Ashizuka and Ishida [67] developed a high strength material (Table 1) with high crystallinity with the eutectic composition (38 wt% TCP and 62 wt% D).

Glasses and glass-ceramics present low toughness (Table 1) and associated lack of crack tolerance. Carefully thermal treated glass and glass-ceramic test specimens with polished surfaces [66] might attain relatively high bending strengths, even comparable to those of bone (Tables 1 and 2), however, the high values of strength are partly due to the preparation of the surface of the specimens to eliminate surface defects which usually cannot be avoided during material processing.

Apart from the lack of mechanical performance, the main drawback of glasses and glass-ceramics for applications as scaffold walls is the difficulty of reproducing the microstructures of optimized test specimens when fabricating porous 3D parts. To overcome this lack, different polycrystalline bioceramics inspired by the bioactive compositions of silicate-based glasses and glass-ceramics in the ternary system TCP-D-W have been proposed. These materials are discussed in which follows.

8. Polycrystalline materials with improved mechanical behavior in the system $Ca_3(PO_4)_2$–$CaSiO_3$–$CaMg(SiO_3)_2$

The knowledge of the $Ca_3(PO_4)_2$–$CaSiO_3$–$CaMg(SiO_3)_2$ system and the excellent results obtained for glasses and glass-ceramics with compositions within this system have been the basis for the development of polycrystalline bioceramics of variable microstructure and different biological and mechanical properties. In Fig. 1 c), the chemical composition of materials studied by different authors are plotted in the ternary system TCP-W-D.

8.1. Single-phase polycrystalline bioceramics

8.1.1. Tricalcium phosphate

The most used calcium orthophosphate materials are based on tricalcium phosphate ($Ca_3(PO_4)_2$). This compound has three different polymorphs [68]: the high temperature ones, α-$Ca_3(PO_4)_2$ and α′-$Ca_3(PO_4)_2$, and the low temperature one, β-$Ca_3(PO_4)_2$. α′-TCP is stable over ≈1430 °C and transforms readily on cooling to α-TCP. β-TCP is stable from room temperature and transforms reconstructively to α-TCP with a volume increase of about 7 %. This transition has been reported to occur at temperatures from 1125 to 1180 °C [68–70]. In general, different reported transition temperatures are associated to different characteristics of the starting powders, processing methodology of the specimens and/or experimental characterization techniques. In the case of the β-α-TCP phase equilibrium relationships, the presence of magnesium, which is a very common impurity in commercial calcium compounds, exerts a remarkable effect, as it enters in solid solution (ss) in TCP [69]. For instance, pure β-TCP dense ceramics can be obtained by sintering at temperatures as high as 1500 °C depending on the level of Mg doping [70,71]. Pure phase α- and β-TCPss ceramics as well as controlled mixtures of α+β-TCPss may be obtained by adequate thermal treating and controlling the amount of Mg present in the precursors used [69].

α-TCP is the major powder constituent of hydraulic bone cements used in dentistry, maxillo-facial surgery and orthopedics. Comprehensive and updated reviews about biodegradable cements for bone regeneration can be found in Refs. [72–75]. Calcium phosphate bone cements (CPCs) are self-setting materials constituted by powder and liquid phases that can be directly injected in the bone defect and/or used as gluing agent. They have attracted increased attention for bone repair since their discovery in the 1980's due to their valuable properties such as biocompatibility, biodegradability, osteoconductivity and osteogenic capabilities, hardening ability through a low-temperature setting reaction and moldability. The biggest advantage of biodegradable bone cements is that they are gradually degraded by chemical dissolution and cell absorption after implantation in the bone defect and finally replaced by the newly formed bone tissue.

In the last couple of decades, bone cements have been extensively applied in the repair and regeneration of tissues due to their properties. Main drawback is their low mechanical performance which limits their application in load bearing regions of bone. Also, the complete in-vivo resorption and replacement of CPC with new bone tissue is still controversial.

The first studies and clinical applications of synthetic β-tricalcium phosphate ceramics were performed during the 1970′s [76,77]. Since then, β-TCP granules and coatings are being successfully used for bone repairing in dentistry maxilla-facial and trauma surgery and nowadays it is the component of several commercial mono- or biphasic bioceramics and composites. Single phase granules of diameters 1–4 mm with a high proportion (60–75 wt%) of relatively large (100–500 μm) and pre-shaped cylinders, blocks and wedges with 30-70 vol% interconnected pores of 100–500 μm diameter are commercially available (e. g: CALCIRESORB, CronOS™). A combination of titanium mesh with β-TCP granules and autologous human adipose-derived mesenchymal stem cells (hAMSCs) has been successfully applied in craniofacial surgery [78]. Future challenges include the displacement of the permanent Ti structure by a completely resorbable scaffold. In this sense, we have proposed the use of composite TCP-D polycrystalline scaffolds as solution due to the excellent mechanical behavior of these composites, as compared to other bioceramics, and tunable bioactivity. Main results on these materials will be discussed in section 8.3.

Well known properties of β-TCP materials are their biocompatibility, bioactivity, osteconductivity, and biodegradability. A comprehensive review on TCP synthesis and biological properties was published by Bohner et al., in 2020 [6]. The degradation rate of β-TCP in acidic conditions is 3–12 times higher than that of HAp [30]. Therefore, its

resorption *in vivo* is cell-mediated, due to the acidification of the environment by cells, especially osteoclasts. The osteoconductive potential of β-TCP has been demonstrated (e.g: Refs. [79–81]) however, no apatite layer has been detected between β-TCP, as initially considered as necessary for a ceramic to be bioactive [22,23]. It has been observed that the surfaces of β-TCP implants become rough and bone grows into the finest surface irregularities. In this way, β-TCP bonds to bone through microanchoring between bone and the rough surface of the resorbed ceramic [79,80]. Such a mechanism would allow the optimization of the biological behavior of β-TCP-based materials manipulating the porous structure and surface roughness [82]. In addition, it has been proposed that the osteoinductive potential can be modulated by the occurrence of concentration gradients between the inner and the outer part of the implanted material. In this sense, large pH calcium and phosphate concentration changes have been observed in β-TCP granules immersed in SBF [83]. The magnitude of such changes was demonstrated to be dependent on particle size, specific surface area, microporosity, and purity of the β-TCP granules. The presence of cracks in the materials would also modify the biological behavior. In some cases, the relatively high resorption rate of β-TCP might impair bone healing due to the sharp chemical conditions of the environment, limiting its clinical application. An adequate ceramic processing of β-TCP single-phase materials and/or its combination with other bioceramics with lower resorption rate might be a way to optimize the implant behavior, as will be discussed in this paper.

One main drawback of β-TCP materials is their poor mechanical behavior as compared to other CaPs such as hydroxyapatite (HAp), which is linked to the characteristics of their microstructures, as discussed below.

As shown in Table 4, experimental Young's modulus values for dense and fine grained β –TCP materials are variable. They range from a value similar to that calculated theoretically by Liang et al. [84] from the crystalline structure to a value 30 % lower. The experimental strength values (Table 4) are much lower than theoretical one expected from the Young's modulus value ($\sigma_t \approx 0.1 \cdot E = 11$ GPa), as usual in real materials that, at minimum have the grain boundaries as defects. In addition, strength of TCP materials is greatly dependent on grain size, as it can be seen by comparison of data from Refs. [85,86] for two materials fabricated using the same powder and with similar levels of density (>99 %); the material with the smallest grain size presented the highest bending strength (≈180 MPa *vs* 150 MPa, Table 4). The strong dependence of strength on grain size and the variability of the Young's modulus is associated to thermal expansion anisotropy of the crystalline lattice. The great crystalline thermal expansion anisotropy of β –TCP ($\alpha_{22-1000^\circ C}$: ≈ 8 and 24 × 10^{-6} K^{-1} for a and b axis, respectively calculated from Ref. [87]) is responsible for such dependence.

When cooling materials with crystalline thermal expansion anisotropy from the sintering temperature, stresses are developed at the boundaries of grains with different orientations due to thermal expansion mismatch. Such stresses lead to cracking for grain sizes larger than the critical one [88], as occurred in β-TCP materials doped with 1 wt% diopside sintered at relatively high temperatures (≈1300-1400 °C) which developed coarse microstructures with crack networks and associated low strengths (DCDT, average strengths ≈ 4–6 MPa, calculated from Weibull distributions in Ref. [89]), as compared to undoped specimens sintered at lower temperatures (DCDT, average strengths ≈ 15, 19 MPa, depending on processing, Fig. 4a)-b) [89], Table 4). In the same way, microcracks are responsible for low values of the Young's modulus. For grains smaller than the critical, the thermal stresses are kept at room temperature as residual stresses that add to the applied ones during use, leading to the relatively low strength presented by β-TCP materials (Table 4). A careful control of the microstructure of ceramics with residual stresses and/or microcracks might lead to better properties. For example (Table 4), average tensile strength (DCDT)

Table 4
Mechanical properties of dense β-TCP based polycrystalline bioceramics.

Material	First author and reference	Strength (MPa)			Young's modulus (GPa)	Fracture Toughness K_{IC} ($MPam^{1/2}$)
		Uniaxial compression	Bending (3 PB)	Tensile DCDT	Dynamic	SEVNB
β-TCP						
	Liang [84]				110[a]	
>99 % T.D. HIP, Transparent	Boilet [85]		181 ± 12		105	1.03 ± 0.09
99 % T.D. d = 0.5–3 μm	Garcia-Prieto [86]		150 ± 30		110 ± 3	0.8[b]
Non-optimized processing	García-Páez [89]			σ_{av} = 15		
Fig. 4a				σ_0 = 17 m = 2		
>99 % T.D d = 0.5–3 μm	Vanhatupa [90]			σ_{av} = 19		
Fig. 4b				σ_0 = 20 m = 8		
SPS	Tkachenko [91]	200.4 ± 10.6		σ_{av}		0.76 ± 0.05[c]
98 % T.D.				28.9 ± 15.0		
β-TCPss						
1300 °C (5 wt% D initial)	García-Páez [89]			σ_{av} = 35		
Fig. 4c				σ_0 = 38 m = 10		
1300 °C (10 wt%D initial)	García-Páez [89]			σ_{av} = 16		
Fig. 4d				σ_0 = 18 m = 4		
β-TCP + 3 wt% HAp						
Porous >2 μm	Hsu [92]	40 ± 8	7.5 ± 0.5 4 PB			
β-TCP/D (wt.%)						
20/80	Vanhatupa [90]			σ_{av} = 72		
				σ_0 = 73 m = 7		
40/60	Vanhatupa [90]			σ_{av} = 63		
≈98 % T.D.				σ_0 = 64 m = 6		
40/60	del Valle García [31]			σ_{av} = 3.9		
Freeze cast ≈ 50 % Open porosity				σ_0 = 4.0 m = 6		
40/60	del Valle García [31]			σ_{av} = 2.4		
Freeze cast + Laser				σ_0 = 2.5 m = 6		

T.D.: theoretical density; HP: Hot pressing; HIP: Hot isostatic pressing; SPS: Spark Plasma Sintering.
[a] Calculated theoretical.
[b] Stable tests.
[c] Indentation; σ_0 and m are the Weibull modulus and characteristic strength, respectively. σ_{av}: average strength.

values of well processed dense β-TCP materials change from ≈ 19 MPa for a conventionally sintered material [90] to ≈ 30 MPa for a submicronic grain size one prepared by spark plasma sintering (SPS) [91]. However, such a sintering technology cannot be used in the case of scaffolds, thus, microstructure has to be optimized by different means.

Thermal expansion mismatch also occurs between grains of different phases with different orientations, in fact, β-TCP as second phase has been reported as detrimental to the mechanical behavior for HAp-β-TCP composites, as reviewed by Wagoner Johnson et al. [32] In Table 4, the extremely low values corresponding to a HAp(3 wt%)-β-TCP material with relatively large grain sizes (>2 μm) [92] are collected as an example.

Ceramic-ceramic composites containing phases with crystalline thermal expansion anisotropy might have improved specific properties once the microstructure is adequately tuned. In this sense, different ceramic-ceramic composites containing β-TCP with sufficient mechanical properties and tailored bioactivity have been developed using compositions in the considered ternary system, as it will be discussed in sections 8.2 and 8.3.

8.1.2. Wollastonite

Until 1991, the glasses and glass-ceramics with CaO, P_2O_5 and SiO_2 as main constituents described previously were the only materials showing the standard concept of bioactivity identified by Hench et al. [22,23] The first to demonstrate that a P_2O_5-free CaO–SiO_2 glass also developed a hydroxyapatite layer during soaking in simulated body fluid (SBF) were Ohura et al. [93] in 1991. This was the basis for the development of polycrystalline wollastonite materials.

The process of formation of the surface hydroxyapatite layer on the surface of bioactive glasses and glass-ceramics (type A bioactivity) starts with the exchange of H_3O^+ ions from the environment for ions existing in the glass or glass ceramic matrix (Na^+, K^+, Ca^{2+}, Mg^{2+}, …etc.). Considering this fact and that the crystalline structure of pseudo-wollastonite (psW; ps-$CaSiO_3$) should permit fast diffusion of H_3O^+ ions from physiological fluid inside the crystal and its exchange with Ca ions, S. de Aza et al. proposed psW as the first bioactive polycrystalline silicate-based ceramic [94]. The *in vitro* bioactivity exhibited by psW was reported by these authors in 1994 [95,96] and further studies demonstrated its type A bioactivity both *in vitro* in human saliva [97] and *in vivo* [98].

Ps-wollastonite is a high temperature polymorph of $CaSiO_3$ that crystalizes in a triclinic lattice [99] and which may exist in metastable state at room temperature. The low temperature form of wollastonite has six polytypes [99,100], being the most usual the monoclinic 2 M one. This crystal structure is that of high aspect ratio natural wollastonite particles used as reinforcing phases in products such as plastics or paint films. Reported temperatures for the 2 M → pseudo wollastonite polymorphic transition in high purity $CaSiO_3$ are slightly different (1130 ± 5 °C [115], 1125°C [99]); the transformation temperature changes in the presence of different ions (e.g: Ca and P [101] and Mg [115]). The presence of Mg in solid solution in wollastonite ($Ca_{1-x}Mg_xSiO_3$; $0 \leq x \leq 0.17$) increases the transition temperature up to ≈1370 °C, which explains the presence of the 2 M form in composites with diopside sintered at high temperatures [115]. The denominations α and β wollastonite are inconsistently used for the high temperature psW and the low temperature 2 M forms depending on the geographic area of the reporting research group. In order to be sure which material is being discussed the best way is to identify the sintering temperature because the 2 M → psW transformation occurs readily in pure materials.

Wollastonite is known to present high bioactivity [115,116], however, it lacks mechanical performance as shown in Table 3. There is only one research [102] that reports strength values of wollastonite material relatively high as compared to HAp or β -TCP (Tables 3 and 4). The material was prepared by SPS at 950 °C, so it would correspond to the low temperature polymorph 2 M, and had fine grains (<1 μm, from the microstructures shown) and high density (95 %). Contrarily, uniaxially pressed compacts from commercial 2 M wollastonite powders, or powders prepared by chemical routes, sintered at temperatures under the transformation temperature present extremely low densities and strength (e.g: ≈50 % porosity, bending strength ≈ 20 MPa [103]). In general, sintering at temperatures over the 2 M → psW transformation produces psW materials that also have low densities and associated low bending strength values (e.g: 40–70 % TD and 20–50 MPa) [103,104].

The high aspect ratio of the 2 M wollastonite particles might be responsible for the difficult sintering of the compacts. Careful conditioning of synthetic and natural psW powders by milling down to ≈ 1–2 μm and conventional sintering allow reaching high density psW materials with increased strength but low reliability (i.e: low Weibull modulus)105 (Table 4) which would reveal low toughness.

As in the case of β-TCP, SPS is not a possible processing route for scaffolds, thus, the highest strengths reported for wollastonite should not be considered when thinking about scaffold walls. In principle, the poor mechanical behavior of conventionally sintered wollastonites impedes their use in single-phase biomaterials. In addition, dissolution of wollastonite in SBF leads to an increase of the pH at the SBF/ceramic interface [105]. Due to the high dissolution rate of this phase, the environment might attain toxic levels *in vivo* compromising osteointegration of the biomaterial in the host bone, thus, limiting the use of psW as single-phase material. Contrarily, wollastonite-containing composite materials with attractive mechanical and biological properties have been developed as it will be described in sections 8.2 and 8.3.

8.1.3. Diopside

As described before, Mg and Si are basic for bone growth and regeneration. Diopside ($CaMg(SiO_3)_2$, D) is a Mg- and Si-containing source for bioceramics. From the biological standpoint, diopside is an attractive biomaterial because it is non-cytotoxic, biocompatible and bioactive *in vitro* and *in vivo*. It was proposed for the first time as biomaterial in 1989 by Nakajima et al. [106,107], who demonstrated the capability of diopside to form hydroxyapatite on its surface when immersed in SBF [106] and to directly bond with bone after 2 weeks of implantation as a block in rabbit mandibula [107]. After 4 week the reaction was finished for the diopside block while it took 12 weeks to attain a similar state for a HAp block in the same conditions. In 1995, Nonami et al. [108] reported the mechanisms of formation of HAp in granules and blocks of diopside *in vitro* and *in vivo*. In the *in vivo* experiments, they observed a close contact between bone and diopside with HAp crystal growth from the diopside surface layer, and continuity between the diopside lattice and that of the new crystals. Laboratory tests using Ca–Mg–Si extracts from a diopside material crystalline ceramics [45] have demonstrated that the ionic products released during its dissolution stimulate *in vitro* cell proliferation, osteogenic differentiation and angiogenesis as compared to tricalcium phosphate. Diopside presents lower rate of Si- ions release than other ceramics such as akermanite and bredigite [45,109].

As single-phase and dense material, diopside has better mechanical behaviour than other bioceramics. As seen in Tables 3 and 4, diopside dense specimens have higher bending strength, Young's modulus and toughness than optimized HAp ((about 3 times) and β-TCP (about 2 times) specimens tested in the same conditions [40]. In the same way, reported compressive strength values of diopside scaffolds (1.4–0.6 MPa, 75–80 % porosity) are higher than those of HAp (<0.3 MPa, 0.69–86 % porosity), 45S5 Bioglass^R (0.6–0.4 MPa, 82–89 % porosity) and $CaSiO_3$ (0.3 MPa, 81 % porosity) scaffolds. [110] The relatively low resorption rate and better mechanical behavior of diopside than those of other bioceramics makes of this compound one ideal candidate for multiphase materials containing highly dissolvable phases and stable phases with improved mechanical behavior, as discussed in sections 8.2. and 8.3.

8.2. Polycrystalline bioceramics in the systems TCP –W and W-D

As discussed above, it is not possible to reach both optimum biological and mechanical performance when considering single-phase TCP, W and D materials. However, each phase has attractive properties to be considered in scaffold walls. Different resorption rates allow to envisage initially dense bioactive ceramic materials capable of developing an *in situ* porous structures once implanted. The adequate mechanical behavior of the low rate resorbing phase would maintain the structural integrity of the scaffold while being colonized by bone. In order to take advantage of and modulate the attractive biological behavior of wollastonite and to avoid its lack of mechanical properties and sinterability, two families of biphasic biomaterials containing wollastonite as a phase have been developed. They have been formulated in the binary systems TCP-W and D-W.

8.2.1. System TCP-W

De Aza et al. were the first to propose a composite material TCP-W, Bioeutectic®, as polycrystalline bioceramic in 1989 [94]. Their initial approach was to overcome the lack of mechanical properties of porous scaffolds by making a material that would develop porosity once implanted, simultaneously to bone colonization. The selected microstructure was that of the eutectic point of the system TCP-W [101] (Fig. 1c, wt.%: ≈40 TCP/60 W and 1402 ± 3 °C) obtained by slow solidification of a melt with the eutectic composition, under a radial gradient of heat extraction. The microstructure is constituted of quasi-spherical colonies of alternated radial lamellae of psW and α-TCP, embedded in highest volume fraction phase, psW. The phase that dissolved preferentially in SBF [94] and human parotid saliva [111] was α-TCP, which initially was expected to be the bioactive phase, and HAp was formed on the psW zones. After sufficient immersion time in SBF, the original microstructure was completely replaced and the final material was constituted by a porous HAp structure with interconnected channel pores of diameter smaller than <1 μm. In spite of the interesting theoretical approach of Bioeutectic®, the material has two main drawbacks to be used in practice for scaffold walls. On the one hand, as massive material for implant blocks, the size of the pores is too small to be colonized by osteoblasts and, on the other hand, the process of slow cooling of a melt is not adequate for the fabrication of scaffolds.

8.2.2. System W-D

In order to avoid the drawbacks of Bioeutectic®, Sainz et al. [115] proposed the eutectic composition of the W-D system (Fig. 1c), wt.%: 36.77 W/63.23 D) focusing materials with the ability of developing a porous structure containing apatite when implanted to provide osseointegration. In principle, the use of solid-state sintering, a conventional ceramic process, would allow the fabrication of different sizes and shapes and the control of macro porosity of such bioceramics when required. The materials studied by these authors were obtained by solid state sintering of synthetized psW and D powders. Depending on the sintering temperature, the materials contained psW (T=1250 and 1300 °C) or W-2M (T=1350 °C) as second phase. The diopside-rich composition was chosen close to that of the eutectic to facilitate sintering at lower temperatures. It was hypothesized that diopside will provide the materials with sufficient structural integrity during bone colonization due to its low resorption rate. Both materials containing psW had relatively large porosities (20–26 vol%) while the material with W-2M had 8 vol% porosity. The high solubility of wollastonite in SBF led to the *in situ* formation of an interconnected porous apatite-like/diopside layer at the ceramic–SBF interface. This porous structure is a three-dimensional architecture ceramic matrix that is expected to be useful for the colonization by cells and new bone formation.

The actual mechanical properties of the W-D materials developed have not been analyzed and the approach has not been implemented for high porosity materials with large pores. However, the conventional ceramic processing route used allows to hypothesized the adequacy of the W-D microstructures proposed for walls of scaffolds.

8.3. Polycrystalline bioceramics in the system TCP-D-W

Phase relations in the $Ca_3(PO_4)_2$–$CaMg(SiO_3)_2$ system were established by Sata112 and revised by Carrodeguas et al. [113] (Fig. 1 d). Sata [112] reported a eutectic point located at 63 wt% $CaMg(SiO_3)_2$ and 1300 ± 5 °C. The existence of this eutectic point was confirmed by Carrodeguas et al. [113], with stoichiometric diopside ($CaMg(SiO_3)_2$) coexisting with β-$[(Ca_{1-x}Mg_x)_3(P_{1-\delta}Si_\delta O_{4-\delta/2})_2]$, indicating the dissolution of D in the TCP network. This dissolution is incongruent, with the smaller Mg^{2+} cation being much more soluble than the bigger Si^{4+}. Thus, even though these authors did not detect any minor phase associated to the Si^{4+} excess, they concluded that the system TCP-D is not a real binary, but a pseudo-binary system in the quaternary system $CaO–P_2O_5–SiO_2–MgO$. For the sake of simplicity, this system has been considered as binary for compositions with low tricalcium phosphate amounts (≤40 wt%), however, our research has consistently demonstrated the presence of wollastonite 2 M in thermally treated TCP-D compositions with diopside amounts from 10 wt%, as will be described later [31,90].

As described previously, synthetic β-tricalcium phosphate ($Ca_3(PO_4)_2$, TCP) granules and coatings are being successfully used for more than 40 years for bone repairing in dentistry, maxilla-facial and

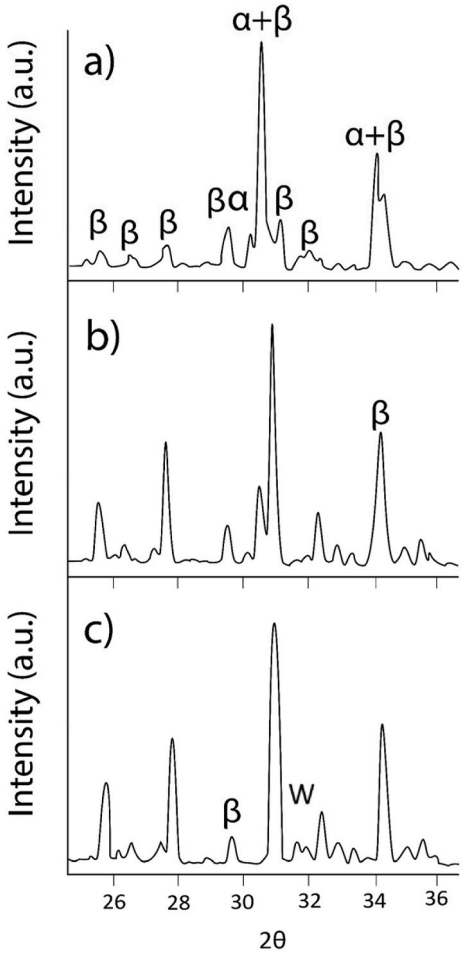

Fig. 3. XRD diffractograms of sintered materials corresponding to TCP-D compositions with 100–90 wt% TCP in the green state plotted in Fig. 1 c) and d).
a) Composition with 100 wt% of TCP sintered at 1300 °C.
b) Composition with 99 wt% of TCP sintered at 1300 °C.
c) Composition with 90 wt% TCP sintered at 1225 °C.

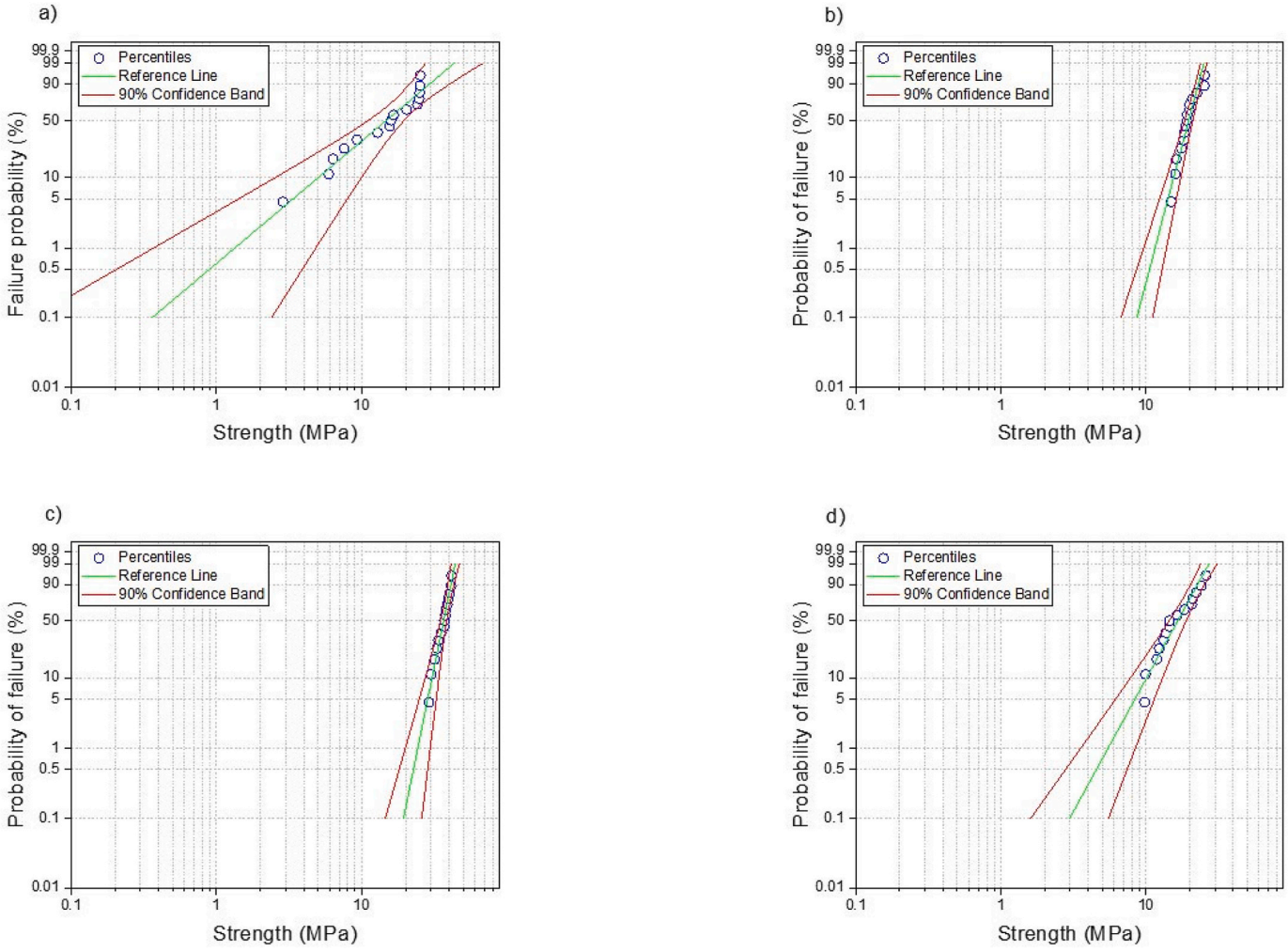

Fig. 4. Weibull distributions of tensile strength values (DCDT) corresponding to single-phase β-TCPss materials.
a) Material with 100 wt% of TCP. Non optimized green processing. Weibull modulus = 2.
b) Material with 100 wt% of TCP. Optimized green processing. Weibull modulus = 8.
c) Material with 95 wt% of TCP. Optimized green processing. Weibull modulus = 10.
d) Material with 90 wt% of TCP. Optimized green processing. Weibull modulus = 4.

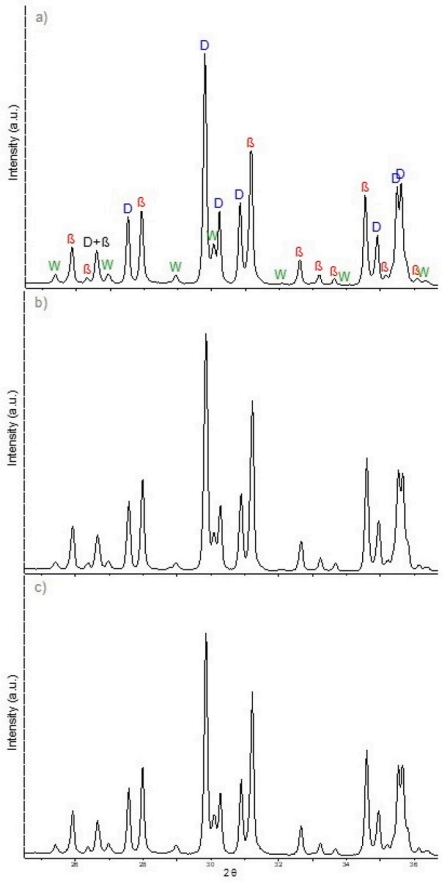

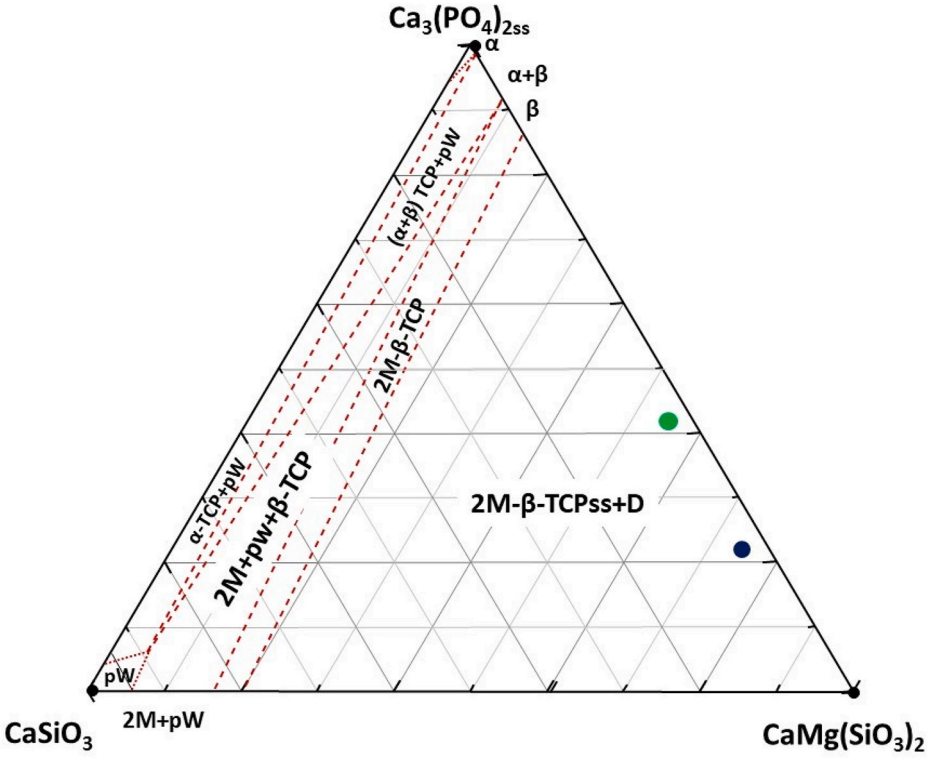

(caption on next page)

Fig. 5. phases found in the TCP-D materials with TCP contents ≤40 wt%.
a)-c) XRD diffractograms of sintered materials (1225 °C) fabricated using different green processing routes. Uniaxial pressing (a); Freeze casting (b); Freeze casting and laser ablation (c).
d) Schematic representation of the solid state compatibility in the TCP-W-D system at 1225 °C. The compositions with TCP = 40 and 20 wt.% are plotted considering the presence of wollastonite.
TCP: $Ca_3(PO_4)_2$; pW: pseudo-wollastonite ($CaSiO_3$); 2 M: wollastonite 2 M; D: diopside ($CaMg(SiO_3)_2$.
Note the significant solid solutions of diopside in wollastonite and TCP that change with composition.

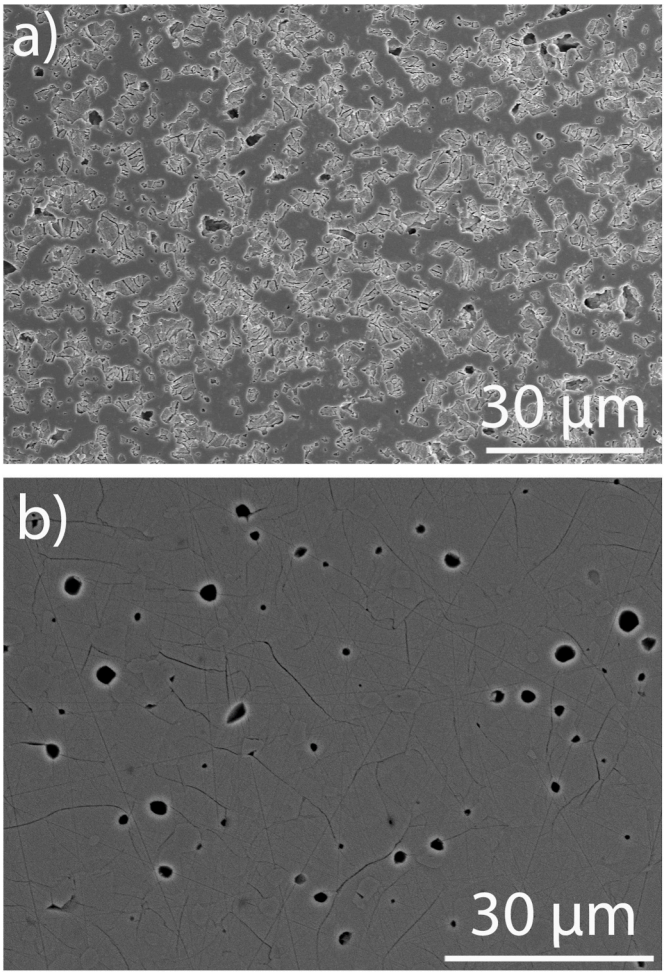

Fig. 6. Characteristic microstructures of materials sintered at 12225 °C.
a) Composition with 40 wt% TCP. Homogeneous microstructure constituted by a diopside matrix surrounding highly microcracked β-TCPss zones is observed.
b) Pure 100 wt% TCP composition. Extensive cracking through the whole microstructure is observed.

trauma surgery. Well known properties of β-TCP materials are their biocompatibility, bioactivity, osteconductivity, and biodegradability. Materials developed in the pseudo-binary system TCP-D present high potential to take advantage of the attractive properties of β-TCP in applications where structural integrity is needed. The adequate biological behavior is assured by the excellent biological behaviour of glasses and glass-ceramics with compositions formulated in this system.

In our group it has been demonstrated that conventional solid-state sintering of green compacts is an adequate method to fabricate materials with different compositions and microstructures in the pseudobinary system TCP-D. The main advantage of such conventional ceramic processing is that it can be scaled for the sintering of green shaped scaffolds. A series of optimized materials were processed using powder conditioning by milling and selected sintering temperatures. We have demonstrated that the phase development in β-TCP-D porous scaffolds processed using different shaping methods is the same as that in dense composites shaped by uniaxial pressing [31]. In Fig. 1 d) the studied chemical compositions are plotted in the binary system TCP-D. Sintered materials containing 40 and 20 wt% TCP in the green state present improved mechanical behavior as compared to single-phase β-TCP, β-TCPss and other bioceramics. In addition, the attained improvement of the mechanical behavior is maintained in the scaffold walls [31]. The main results are described below.

Preliminary works showed that sintered materials with green compositions (wt.% of TCP) from 100 to 40 are biocompatible and not cytotoxic to human osteoblasts and stimulate cell proliferation increasingly with silicon content [89,114].

XRD diffraction patterns of sintered materials with TCP 90–100 wt% are shown in Fig. 3. The sintered TCP (1300 °C) 100 and 99 wt% compositions were a mixture of α and β-TCP, as expected from the TCP-D system (Fig. 1 d)). The composition with 95 wt% of TCP led to an essentially single-phase thermally treated (1250 °C) material with diopside in solid solution, β-TCPss, also expected from the binary diagram, while traces of wollastonite were detected in the 90 wt% TCP composition. The Weibull distributions of the tensile strength (DCDT) values of these materials are plotted in Fig. 4. Adequate conditioning of the TCP powder by milling leads to a significant increase in the reliability of the pure single-phase β-TCP material, as revealed by the sharp increase of the Weibull modulus (x4, Fig. 4 a)-b)), however, strength values remain relatively low ($\sigma_0 \approx 20$ MPa, Fig. 4 a)-b)). Optimized processing of the 95 wt% TCP composition led to β-TCPss sintered specimens with significantly higher values of strength ($\sigma_0 \approx 38$ MPa, Fig. 4 c)) and slightly higher reliability (Weibull modulus ≈ 8 and 10 for β-TCP and β-TCPss, respectively). However, higher amounts of diopside led to the degradation of the mechanical behavior (Fig. 4 d)) due to the coarsening of the microstructure and associated cracking [89].

For lower amounts of TCP (20 and 40 wt%) the sintered materials were constituted by β-TCPss and diopside as major phases and small amounts of wollastonite ($CaSiO_3$, W; ≈6 wt% for 40 wt% TCP) [31]. As an example, Fig. 5 a)-c) shows the XRD difractograms of materials with 40 wt% TCP green processed using different routes and sintered at the optimum sintering temperature, 1225 °C. The presence of W as third phase is due to the incongruent dissolution of diopside in the TCP described above. The real phase composition of these high diopside-containing materials has to be plotted in the ternary system TCP-W-D, as shown in the isothermal section at 1225 °C (Fig. 5 d)). Wollastonite is a highly bioactive ceramic compound, as described above [6,11,115]. Diopside resorption is slower than that of β-TCP and presents much higher toughness and stiffness (Tables 3 and 4), thus, suitable microstructural design allows the tailoring of bioactivity and mechanical response of materials in the TCP-D system. Optimum mechanical behavior was obtained for materials with the lowest amounts of TCP (40–20 wt%).

Optimized (thermal treatment and powder conditioning) processing of mixtures with green compositions (β-TCP/D wt.%) 20/80 and 40/60 uniaxially pressed and sintered produce homogeneous materials constituted by a diopside matrix surrounding highly microcracked β-TCPss zones and some isolated wollastonite particles [90]. Fig. 6 a) shows the characteristic microstructure of these composites. In the single-phase β-TCP material processed similarly, cracks are not confined into certain areas but traverse the whole material (Fig. 6 b)) When mechanically loaded, fracture origins are the TCP areas and microcrack growth is limited by the tough diopside matrix which presented transgranular fracture [90]. This mechanism endows the composite materials

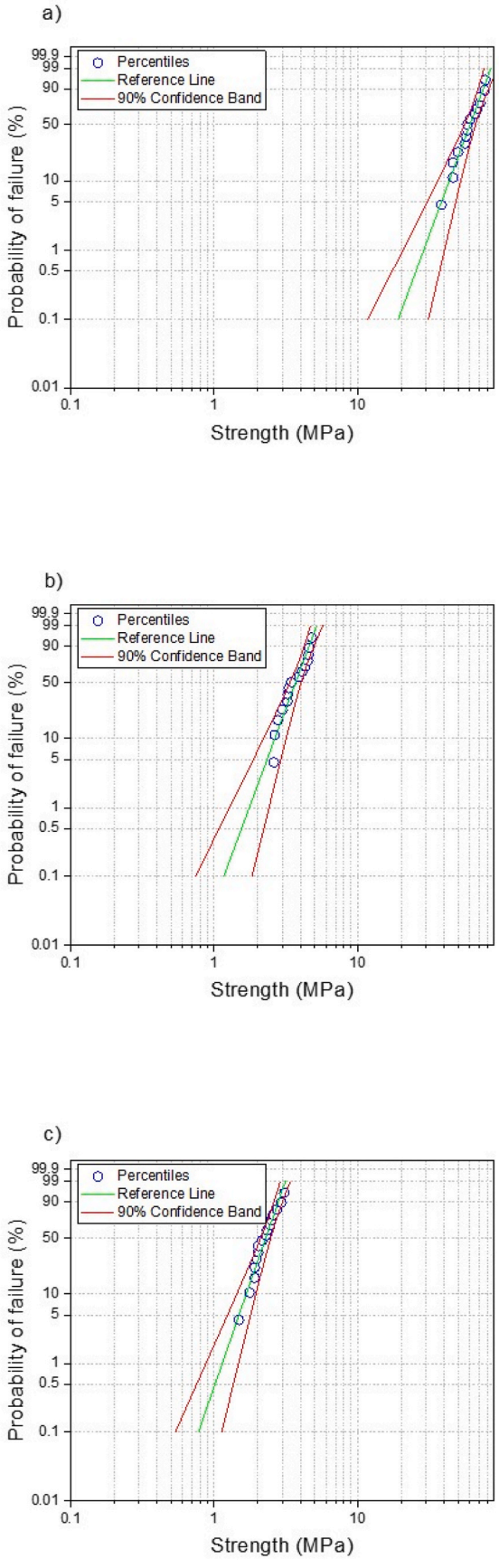

(caption on next column)

Fig. 7. Weibull distributions of tensile strength (DCDT) for sintered (1225 °C) materials with TCP contents ≤40 wt% fabricated using different green processing routes. The Weibull parameters are summarized in table 4.
a) Uniaxial pressing, P.
b) Freeze casting, FC.
c) Freeze casting and laser ablation, FC + L.
As FC and FC + L specimens were bigger than the P ones, strength values have been corrected using the Weibull modulus (m = 6) and the effective volume to be comparable to data for the P specimens.

with higher strength (>3x) compared to single-phase TCP and reliability similar to that of the optimized single-phase β-TCP (Fig. 7 a) and 4 b), Table 4). In addition, tensile strength values of these specimens are in the range of those of cortical skull bone (Table 1).

The improved mechanical behavior due to the presence of diopside is maintained in the walls of highly porous scaffolds, as it was demonstrated for the composition with 40 wt% of TCP using two kinds of model specimens with different levels and morphology of pores [31]. This composition was chosen for scaffolds because of its higher bioactivity [90]. One series of porous specimens (FC) was fabricated using freeze casting by ice templating. Porosity in freeze cast has been demonstrated to be adequate for the colonization by osteoblasts [117]. Another series (FC + L) was prepared by laser ablation of the green porous FC specimens to reach large cylindrical pores capable for vascularization.

The Weibull strength distributions for the porous scaffolds prepared using freeze cast (FC) and freeze cast and subsequent laser ablation (FC + L) are plotted in Fig. 7 b)-c), compared to the distribution for the uniaxially pressed specimens (P, Fig. 7 a)). Considering the simplified model of a bidimensional cellular porous microstructure uniaxially loaded [118] it is possible to evaluate the strength of the wall of the FC specimens using the experimental values of strength and the open porosity. For σ≈4 MPa (Fig, 7 b), Table 4) The obtained value, ≈50 MPa, is in the range of the corresponding to pressed specimens (≈60 MPa) showing that the relatively good mechanical behavior of the microstructure of pressed specimens is kept in the scaffolds. In addition, preliminary results [119] for specimens with ≈8 % open porosity sintered from green parts fabricated by Lithoz GMBH the Lithography-based Ceramic Manufacturing (LCM) have shown that the phase development is similar to that of specimens shaped by the other methods (wt.% ≈ 57, 38 and 5 of D, β-TCPss and W, respectively) and that they maintain the reinforcing effect of diopside which keeps its transgranular fracture mode.

Both structures with high porosity, FC and FC + L, have tensile strengths (Table 4) in the range or even higher of most values of compressive strength reported for cancellous bone (Table 1), thus, sufficient for scaffold performance [27,34], as discussed in section 4.

The single-phase β-TCP and the β-TCPss-D composites have excellent bioactive behavior [90], as they support viability and osteogenic differentiation of human mesenchymal stem cells (hASCs). Main difference is the process of cell colonization and resorption of the materials. Modifications of the single-phase material occur homogeneously in the surface where a uniform and continuous layer of cells form (Fig. 8 a)). Initially, cell colonization in the composites (Fig. 8 b)-c)) occurs through the microcracked β-TCPss which is preferentially resorbed leaving the structure of diopside surrounded by the cell layer that enters into the material. This specific morphological features of the colonization of the materials by hASCs permits to infer that in the composite scaffolds seeded with hASC, the initial bone structure would be generated while maintaining the structural integrity of the scaffold. The remaining diopside will be resorbed for longer times as the bone structure grows further. In addition, the differential resorption rate of the mechanically performant phase diopside will permit cell seeding of the scaffold *in vitro* without compromising scaffold architecture.

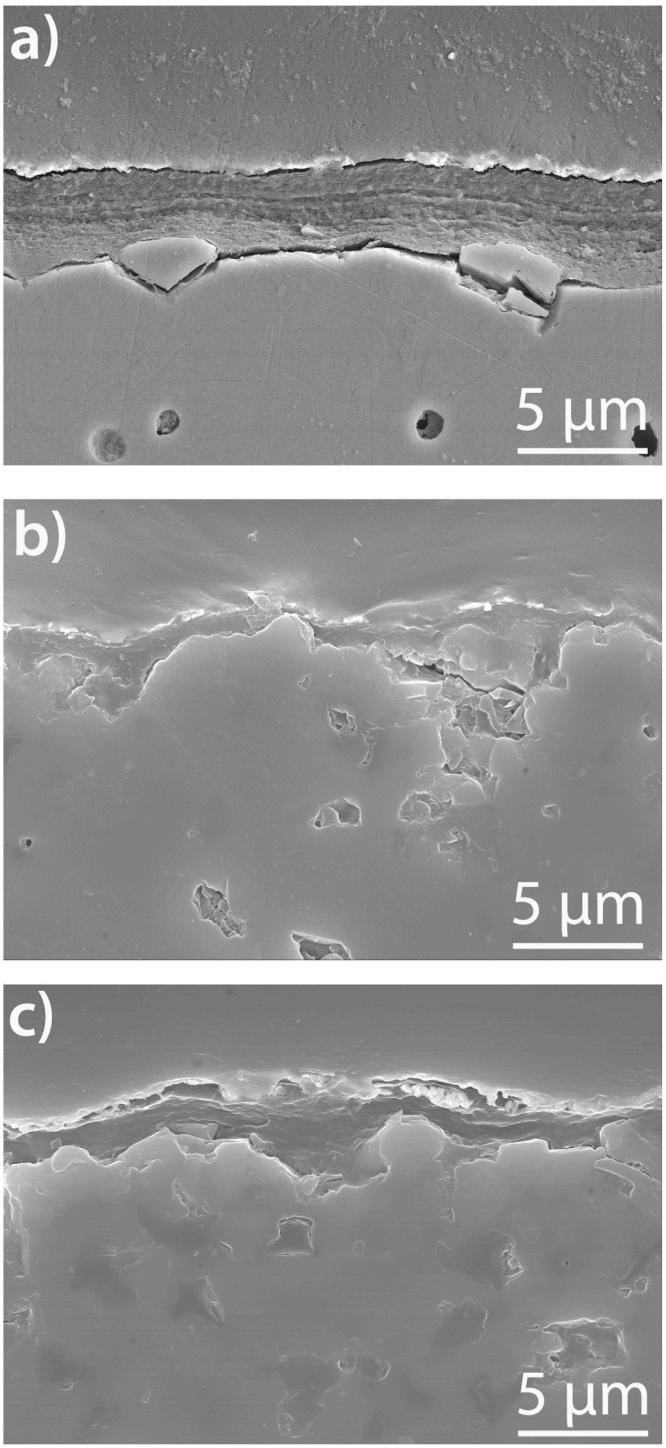

Fig. 8. Cell colonization in materials sintered at 1225 °C.
a) Pure 100 wt% TCP composition.
b) Composition with 40 wt% TCP.
c) Composition with 20 wt% TCP.

9. Concluding remarks

Modern perspectives for bone repairing and regeneration are based on the use of engineered structures combining resorbable bioceramic scaffolds, cells and/or reactive agents as growth factors or antibiotics: tissue engineering constructs (TEC). In the ideal case, these structures would facilitate host cells to deposit extracellular matrix (ECM) and replace the scaffold structure over time.

Bones with different function differ strongly in shape and structure. One main opportunity for ceramic scaffolds is in the repair of plate-like bones, where the mechanical solicitations are lower and specific forms that can be green shaped by 3D technologies are required.

Bioceramics for scaffolds should combine properties needed for adequate cellular function and viability and sufficient mechanical strength. The challenge is materials constituted by highly dissolvable phases and low resorbing phases with improved mechanical behavior. Layered or gradient porous structures with optimum behavior due to the contribution of the different layers could also be envisaged.

Multiphase polycrystalline ceramics in the system TCP-W-D are one of the most appropriate responses to such a challenge. Solid-state sintered bioceramics of variable microstructure and adequate biological and mechanical properties have been developed. Composites with TCPss microcracked areas surrounded by diopside present high strength due to the mechanically performant phase diopside. The differential resorption rate of diopside permits cell seeding of the scaffold *in vitro* without compromising scaffold architecture. The main advantage of such conventional thermal treatment is that it can be scaled for the sintering of green porous scaffolds shaped by different methods. Results reviewed in this paper open a wide opportunity of developing personalized resorbable scaffolds for bone regeneration.

Declaration of competing interest

The authors declare that they have no known competing financial interests or personal relationships that could have appeared to influence the work reported in this paper.

Acknowledgements

The findings of our group described in this paper are the results of collaborations through the years. The work performed in Spain has been funded by the Spanish Ministry of Science and Innovation and by CSIC. Specific projects are acknowledged in the cited papers.

International collaborations have been performed in the frame of the COST Action MP1301, NEWGEN. Special thanks to our colleagues from the Adult Stem Cell Group of the Faculty of Medicine and Health Technology of Tampere University (Finland), CRIBC (Belgium), LMCPA (France) and Lithoz GmbH (Austria).

Ph. D. students: M. Magallanes-Perdomo and A. García-Prieto, supported by the Ministry of Science and Innovation of Spain, and I. H. García-Páez (Universidad Francisco de Paula Santander, Colombia) supported by COLCIENCIAS.

References

[1] G.L. Koons, M. Diba, A.G. Mikos, Materials design for bone- tissue engineering, Nature Reviews, Nature Reviews | MATERIALS 5 (2020) 584–603, https://doi.org/10.1038/s41578-020-0204-2.
[2] G. Turnbull, J. Clarke, F. Picard, P. Riches, L. Jia, F. Han, B. Li, W. Shu, 3D bioactive composite scaffolds for bone tissue engineering, Bioact. Mater. 3 (2018) 278–314, https://doi.org/10.1016/j.bioactmat.2017.10.001.
[3] V.P. Galván-Chacóna, D. de Melo Pereira, S. Vermeulen, H.YuanbJ. Li, P. Habibović, Decoupling the role of chemistry and microstructure in hMSCs response to an osteoinductive calcium phosphate ceramic, Bioact. Mater. 19 (2023) 127–138, https://doi.org/10.1016/j.bioactmat.2022.03.030.
[4] S. Dorozhkin, Bioceramics of Calcium Orthophosphates, Biomaterials 31 (2010) 1465–1485, https://doi.org/10.1016/j.biomaterials.2009.11.050.
[5] W. Suchanek, M. Yoshimura, Processing and properties of hydroxyapatite-based biomaterials for use as hard tissue replacement implants, J. Mater. Res. 13 (1998) 94–117, https://doi.org/10.1557/JMR.1998.0015.
[6] Bohner, B.L. Santoni, N. Dobelin, β-tricalcium phosphate for bone substitution: synthesis and properties, Acta Biomater. 113 (2020) 23–41, https://doi.org/10.1016/j.actbio.2020.06.022.
[7] R.Z. LeGeros, S. Lin, R. Rohanizadeh, D. Mijares, J.P. LeGeros, Biphasic calcium phosphate bioceramics: preparation, properties and applications, J. Mater. Sci. Mater. Med. 14 (2003) 201–209.
[8] G.R. Owen, Rh Gethin, M. Dard, H. Larjava, Hydoxyapatite/β-tricalcium phosphate biphasic ceramics as regenerative material for the repair of complex bone defects, J. Biomed. Mater. Res. Part B: Materials in medicine 106 (2018) 2493–2512, https://doi.org/10.1002/jbm.b.34049.

[9] M. Bouler, P. Pilet, O. Gauthier, E. Verron, Biphasic calcium phosphate ceramics for bone reconstruction: a review of biological response, Acta Biomater. (2017) 1–12, https://doi.org/10.1016/j.actbio.2017.01.076.

[10] M. Magallanes-Perdomo, A.H. De Aza, I. Sobrados, J. Sanz, P. Pena, Structure and properties of bioactive eutectic glasses based on the $Ca_3(PO_4)_2$–$CaSiO_3$–$CaMg(SiO_3)_2$ system, Acta Biomater. 8 (2012) 820–829, https://doi.org/10.1016/j.actbio.2011.10.017.

[11] M. Mellor, I. Hawkes, Measurement of tensile strength by diametral compression of discs and annuli, Eng. Geol. 5 (1971) 173–225, https://doi.org/10.1016/0013-7952(71)90001-9.

[12] J.H. Clifford Lee, B. Ondruschka, L. Falland-Cheung, M. Scholze, N. Hammer, D. C. Tong, J.N. Waddell, An investigation on the correlation between the mechanical properties of human skull bone, its Geometry,Microarchitectural properties, and water content, Hindawi Journal of Healthcare Engineering (2019). Article ID 6515797, 8 pages.

[13] K.J. Koester, J.W. Ager III, R.O. Ritchie, The true toughness of human cortical bone measured with realistically short cracks, Nat. Mater. 7 (2008) 672–677, https://doi.org/10.1038/nmat2221.

[14] P. Fratzl, R. Weinkamer, Nature's hierarchical materials, Prog. Mater. Sci. 52 (2007) 1263–1334, https://doi.org/10.1016/j.pmatsci.2007.06.001.

[15] J.D. Currey, The mechanical properties of bone, Clin. Orthop. Relat. Res. 73 (1970) 210–231.

[16] J.H. McElhaney, J.L. Fogle, J.W. Melvin, R.R. Haynes, V.L. Roberts, N.M. Alem, Mechanical properties of cranial bone, J. Biomech. 3 (1970) 495–511.

[17] D. Dapaah, T. Willett, A critical evaluation of cortical bone fracture toughness testing methods, J. Mech. Behav. Biomed. Mater. 134 (2022) 105419, https://doi.org/10.1016/j.jmbbm.2022.105419.

[18] L.L. Hench, Bioceramics, J. Am. Ceram. Soc. 81 (1998) 1705–1728.

[19] L.L. Hench, I. Thompson, Twenty-first century challenges for biomaterials, J. R. Soc. Interface 7 (2010), https://doi.org/10.1098/rsif.2010.0151.focus. S379–9.

[20] M.L. Wickramasinghe, G.J. Dias, K.M.G.P. Premadasa, A novel classification of bone graft materials, J. Biomed. Mater. Res. 110 (2022) 1724–1749, https://doi.org/10.1002/jbm.b.35029.

[21] F. Inchingolo, D. Hazballa, A.D. Inchingolo, G. Malcangi, G. Marinelli, A. Mancini, M.E. Maggiore, I.R. Bordea, A. Scarano, M. Farronato, G.M. Tartaglia, F. Lorusso, A.M. Inchingolo, G. Dipalma, Innovative concepts and recent breakthrough for engineered graft and constructs for bone regeneration: a literature systematic review, Materials 15 (2022) 1120, https://doi.org/10.3390/ma15031120.

[22] L.L. Hench, R.J. Splinter, W.C. Allen, T.K. Greenlee Jr., Bonding mechanisms at the interface of ceramic prosthetic materials, J. Biomed. Mater. Res. 2 (1971) 117–141.

[23] S.F. Hulbert, J.C. Bokros, L.L. Hench, J. Wilson, G. Heimke, Ceramics in clinical applications: past, present, and future, in: P. Vincenzini (Ed.), High Tech Ceramics, Elsevier, Amsterdam, The Netherlands, 1987, pp. 189–213.

[24] L.L. Hench, Bioactive glass bone grafts: history and clinical applications, in: I. Antoniac (Ed.), Handbook of Bioceramics and Biocomposites, Springer, Cham, 2015, https://doi.org/10.1007/978-3-319-09230-0_5-1.

[25] L. Hench, Bioceramics: from concept to clinic, J. Am. Ceram. Soc. 74 (1991) 1487–1510, https://doi.org/10.1111/j.1151-2916.1991.tb07132.x.

[26] L.L. Hench, Biomaterials, Science 208 (1980) 826–831, https://doi.org/10.1126/science.6246576.

[27] I.D. Thompson, L.L. Hench, Mechanical properties of bioactive glasses, glass-ceramics and composites, Proc. Inst. Mech. Eng. H. 212 (1998) 127–136. https://doi/10.1243/0954411981533908.

[28] S.V. Dorozhkin, Calcium orthophosphate (CaPO4) scaffolds for bone tissue engineering applications, Journal of Biotechnology and Biomedical Science 1 (3) (2018) 1–25. https://doi/10.14302/issn.2576-6694.jbbs-18-2143.

[29] M. Bohner, L. Galea, N. Doebelin, Calcium phosphate bone graft substitutes: failures and hopes, J. Eur. Ceram. Soc. 32 (2012) 2663–2671, https://doi.org/10.1016/j.jeurceramsoc.2012.02.028.

[30] D.W. Hutmacher, J.T. Schantz, C.X. Lam, K.C. Tan, T.C. Lim, State of the art and future directions of scaffold-based bone engineering from a biomaterials perspective, J. Tissue Eng. Regen. M. 1 (2007) 245–260. https://doi/10.1002/term.24.

[31] A. del Valle García, D. Hautcoeur, A. Leriche, F. Cambier, C. Baudín, Microstructural design of ceramics for bone regeneration, J. Eur. Ceram. Soc. 40 (2020) 2555–2565, https://doi.org/10.1016/j.jeurceramsoc.2019.10.039.

[32] A.J. Wagoner Johnson, B.A. Herschler, A review of the mechanical behavior of CaP and CaP/polymer composites for applications in bone replacement and repair, Acta Biomater. 7 (2011) 16–30. https://doi/10.1016/j.actbio.2010.07.012.

[33] W. Habraken, P. Habibovic, M. Epple, M. Bohner, Calcium phosphates in biomedical applications: materials for the future? Mater. Today 19 (2016) 69–87, https://doi.org/10.1016/j.mattod.2015.10.008.

[34] T. Kokubo, H.-M. Kim, M. Kawashita, Novel bioactive materials with different mechanical properties, Biomaterials 24 (2003) 2161–2175, https://doi.org/10.1016/S0142-9612(03)00044-9.

[35] F. Albee, H. Morrison, Studies in bone growth, Ann. Surg. 71 (1920) 32–38.

[36] S.V. Dorozhkin, A detailed history of calcium orthophosphates from 1770s till 1950, Mater. Sci. Eng. C 33 (2013) 3085–3110, https://doi.org/10.1016/j.msec.2013.04.002.

[37] O.A. Pinto, A. Tabaković, T.M. Goff, Y. Liu, J.H. Adair, Calcium phosphate and calcium phosphosilicate mediated drug delivery and imaging, p713-744, in: A. Prokop (Ed.), Intracellular Delivery: Fundamentals and Applications, Fundamental Biomedical Technologies 5, © Springer Science+Business Media B. V, 2011, https://doi.org/10.1007/978-94-007-1248-5_23.

[38] L.C. Chow, Development of self-Setting calcium phosphate cements, J. Ceram. Soc. Jpn. 99 (1991) 954–964, https://doi.org/10.2109/jcersj.99.954.

[39] R. Halouani, D. Bernache-Assolant, E. Champion, A. Ababou, Microstructure and related mechanical properties of hot pressed hydroxyapatite ceramics, J. Mater. Sci. Mater. Med. 5 (1994) 563–568, https://doi.org/10.1007/BF00124890.

[40] T. Nonami, S. Tsutsumi, Study of diopside ceramics for biomaterials, J. Mater. Sci. Mater. Med. 10 (1999) 475–479.

[41] A.V. Do, B. Khorsand, S.M. Geary, A.K. Salem, 3D Printing of scaffolds for tissue regeneration applications, Adv. Healthcare Mater. 4 (2015) 1742–1762. https://doi/10.1002/adhm.201500168.

[42] A. Hoppe, N.S. Güldal, A.R.A. Boccaccini, A review of the biological response to ionic dissolution products from bioactive glasses and glass-ceramics, Biomaterials 32 (2011) 2757–2774, https://doi.org/10.1016/j.biomaterials.2011.01.004.

[43] Y.L. Zhou, C.T. Wu, J. Chang, Bioceramics to regulate stem cells and their microenvironment for tissue regeneration, Mater, Today Off. 24 (2019) 41–56, https://doi.org/10.1016/j.mattod.2018.07.016.

[44] A.M.P. Romani, Magnesium in health and disease, in: A. Sigel, H. Sigel, R. Sigel (Eds.), Interrelations between Essential Metal Ions and Human Diseases. Metal Ions in Life Sciences, Springer, Dordrecht, 2013, https://doi.org/10.1007/978-94-007-7500-8_14, 2013.

[45] W. Zhai, H. Lu, C. Wu, L. Chen, X. Lin, K. Naoki, G. Chen, J. Chang, Stimulatory effects of the ionic products from Ca–Mg–Si bioceramics on both osteogenesis and angiogenesis in vitro, Acta Biomater. 9 (2013) 8004–8014, https://doi.org/10.1016/j.actbio.2013.04.024.

[46] M. Ojansivu, S. Vanhatupa, L. Björkvik, H. Häkkänen, M. Kellomäki, R. Autio, J. A. Ihalainen, L. Hupa, S. Miettinen, Bioactive glass ions as strong enhancers of osteogenic differentiation in human adipose stem cells, Acta Biomater. 21 (2015) 190–203, https://doi.org/10.1016/j.actbio.2015.04.017.

[47] L.H. Chen, L. Liu, C.T. Wu, R.Q. Yang, J. Chang, X. Wei, The extracts of bredigite bioceramics enhanced the pluripotency of human dental pulp cells, J. Biomed. Mater. Res., Part A 105 (2017) 3465–3474, https://doi.org/10.1002/jbm.a.36191.

[48] W. Zhai, H. Lu, L. Chen, X. Lin, Y. Huang, K. Dai, K. Naoki, G. Chen, J. Chang, Silicate bioceramics induce angiogenesis during bone regeneration, Acta Biomater. 8 (2012) 341–349, https://doi.org/10.1016/j.actbio.2011.09.008.

[49] M. Diba, O.M. Goudouri, F. Tapia, A.R. Boccaccini, Magnesium-containing bioactive polycrystalline silicate-based ceramics and glass-ceramics for biomedical, Curr. Opin. Solid State Mater. Sci. 18 (2014) 147–168, https://doi.org/10.1016/j.cossms.2014.02.004.

[50] C.R. Howlett, H. Zreiqat, Y. Wu, D.W. McFall, D.R. McKenzi, Effect of ion modification of commonly used orthopedic materials on the attachment of human bone-derived cells, J. Biomed. Mater. Res. 45 (1999) 45–54, https://doi.org/10.1002/(SICI)1097-4636(19990615)45:4<345::AID-JBM9>3.0.CO;2-J.

[51] H. Zreiqat, P. Evans, C.R. Howlett, Effect of surface chemical modification of bioceramic on phenotype of human bone-derived cells, J. Biomed. Mater. Res. 44 (1999) 389–396, https://doi.org/10.1002/(SICI)1097-4636(19990315)44:4<389::AID-JBM4>3.0.CO;2-O.

[52] Y. Huang, C. Wu, X. Zhang, J. Chang, K. Dai, Regulation of immune response by bioactive ions released from silicate bioceramics for bone regeneration, Acta Biomater. 66 (2018) 81–92.

[53] P.N. De Aza, A.H. De Aza, P. Pena, S. De Aza, Bioactive glasses and glass-ceramics, Bol. Soc. Esp. Ceram. V. 46 (2007) 45–55.

[54] A. Shearer, M. Montazerian, J.C. Mauro, Modern definition of bioactive glasses and glass-ceramics, J. Non-Cryst. Solids 608 (2023) 122228, https://doi.org/10.1016/j.jnoncrysol.2023.122228.

[55] O. Peitl, E.D. Zanotto, F.C. Serbena, L.L. Hench, Compositional and microstructural design of highly bioactive P_2O_5–Na_2O–CaO–SiO_2 glass-ceramics, Acta Biomater. 8 (2012) 321–332, https://doi.org/10.1016/j.actbio.2011.10.014.

[56] A. Shearer, M. Montazerian, J.J. Sly, R.G. Hill, J.C. Mauro, Trends and perspectives on the commercialization of bioactive glasses, Acta Biomater. 160 (2023) 14–31, https://doi.org/10.1016/j.actbio.2023.02.020.

[57] A. Goel, S. Kapoor, R.R. Rajagopal, M.J. Pascual, H.W. Kim, J.M.F. Ferreira, Alkali-free bioactive glasses for bone tissue engineering: a preliminary investigation, Acta Biomater. 8 (2012) 361–372, https://doi.org/10.1016/j.actbio.2011.08.026.

[58] S. Kapoor, Â. Semitela, A. Goel, Y. Xiang, Y.J. Du, A.H. Lourenço, D.M. Sousa, P. L. Granja, J.M.F. Ferreira, Uderstanding the composition–structure–bioactivity relationships in diopside ($CaO{\cdot}MgO{\cdot}2SiO_2$)–tricalcium phosphate ($3CaO{\cdot}P_2O_5$) glass system, Acta Biomater. 15 (2015) 210–226, https://doi.org/10.1016/j.actbio.2015.01.001.

[59] T. Kokubo, Bioactive glass-ceramics, in: T. Kokubo (Ed.), Bioceramics and Their Clinical Applications, Woodhead Publishing in Materials, 2008, pp. 284–301, https://doi.org/10.1533/9781845694227.2.284.

[60] S. Teixeira, M. Magallanes, A.H. De Aza, A.Y. Mateus, M.A. Rodríguez, P. Pena, M.P. Ferraz, S. De Aza, F.J. Monteiro, Cell culture studies on hydroxyapatite and wollastonite tricalcium phosphate-based materials for tissue engineering, ECM VIII, European Cell &Materials Meeting: bone Tissue Engineering, Davos, Swiss (June 25-28, 2007).

[61] M. Magallanes-Perdomo, Z.B. Luklinska, A.H. De Aza, R.G. Carrodeguas, S. De Aza, P. Pena, Bone-like forming ability of apatite–wollastonite glass ceramic, J. Eur. Ceram. Soc. 31 (2011) 1549–1561, https://doi.org/10.1016/j.jeurceramsoc.2011.03.007.

[62] M. Magallanes-Perdomo, P. Pena, P.N. De Aza, R.G. Carrodeguas, M. A. Rodríguez, X. Turrillas, S. De Aza, A.H. De Aza, Devitrification studies of wollastonite–tricalcium phosphate eutectic glass, Acta Biomater. 5 (2009) 3057–3066, https://doi.org/10.1016/j.actbio.2009.04.026.

[63] S. Kapoor, A. Goel, M.J. Pascual, J.M.F. Ferreira, Alkali-free bioactive diopside–tricalcium phosphate glass-ceramics for scaffold fabrication: sintering and crystallization behaviours, J.Non-Crystalline Solids 432 (2016) 81–89, https://doi.org/10.1016/j.jnoncrysol.2015.05.033. Part A.

[64] T. Kitsugi, T. Yamamuro, T. Nakamura, T. Kokubo, M. Takagi, T. Shibuya, H. Takeuchi, M. Ono, Bonding behavior between two bioactive ceramics in vivo, J. Biomed. Mater. Res. 21 (1987) 1109–1123, https://doi.org/10.1002/jbm.820210905.

[65] G. Kaur, V. Kumar, F. Baino, J.C. Mauro, G. Pickrell, I. Evans, O. Bretcanu, Mechanical properties of bioactive glasses, ceramics, glass-ceramics and composites: state-of-the-art review and future challenges, Mater. Sci. Eng. C 104 (2019), 109895, https://doi.org/10.1016/j.msec.2019.109895.

[66] T. Kokubo, S. Ito, M. Shigermatsu, S. Sakka, Y. Yamamuro, Mechanical-properties of a new type of apatite-containing glass ceramic for prosthetic application, J. Mater. Sci. 20 (1985) 2001–2004.

[67] M. Ashizuka, E. Ishida, Mechanical properties of silicate glass-ceramics containing tricalcium phosphate, J. Mater. Sci. 32 (1997) 185–188.

[68] R.G. Carrodeguas, S. De Aza, Review. α-Tricalcium phosphate: synthesis, properties and biomedical applications, Acta Biomater. 7 (2011) 3536–3546, https://doi.org/10.1016/j.actbio.2011.06.019.

[69] R.G. Carrodeguas, A.H. De Aza, X. Turrillas, P. Pena, S. De Aza, New approach to the β→ α polymorphic transformation in magnesium-substituted tricalcium phosphate and its practical implications, J. Am. Ceram. Soc. 91 (2008) 1281–1286, https://doi.org/10.1111/j.1551-2916.2008.02294.x.

[70] R. García Carrodeguas, A.H. De Aza, X. Turrillas, P. Pena, Salvador De Aza, New approach to the α-β polymorphic transformation in magnesium-substituted tricalcium phosphate and its practical implications, J. Am. Ceram. Soc. 91 (2008) 1281–1286, https://doi.org/10.1111/j.1551-2916.2008.02294.x.

[71] N. Somers, F. Jean, M. Lasgorceix, H. Curto, G. Urruth, A. Thuault, F. Petit F, A. Leriche, Influence of dopants on thermal stability and densification of β-tricalcium phosphate powders, Open Ceram 7 (2021), 100168, https://doi.org/10.1016/j.oceram.2021.100168.

[72] S.V. Dorozhkin, Calcium orthophosphate cements for biomedical application, J. Mater. Sci. 43 (2008) 3028–3057, https://doi.org/10.1007/s10853-008-2527-z.

[73] O. Demir-Oguz, A.R. Boccaccini, D. Loca, Injectable bone cements: what benefits the combination of calcium phosphates and bioactive glasses could bring? Bioact. Mater. 19 (2023) 217–236, https://doi.org/10.1016/j.bioactmat.2022.04.007.

[74] D. Liu, C. Cui, W. Chen, J. Shi, B. Li, S. Chen, Biodegradable cements for bone regeneration, J. Funct. Biomater. 14 (2023) 134, https://doi.org/10.3390/jfb14030134.

[75] M. Bohner, Calcium orthophosphates in medicine: from ceramics to calcium phosphate cements, Injury, Int. J. Care Injured 3 I (2000), https://doi.org/10.1016/S0020-1383(00)80022-4. S-D37-47.

[76] H.U. Cameron, I. Macnab, R.M. Pilliar, Evaluation of a biodegradable ceramic, J. Biomed. Mater. Res. 11 (1977) 179–186, https://doi.org/10.1002/jbm.820110204.

[77] M. Jarcho, R.L. Salsbury, M.B. Thomas, R.H. Doremus, Synthesis and fabrication of β-tricalcium phosphate (whitlockite) ceramics for potential prosthetic applications, J. Mater. Sci. 14 (1979) 142–150.

[78] K. Sándor, V.J. Tuovinen, J. Wolff, M. Patrikoski, J. Jokinen, E. Nieminen, B. Mannerström, O.-P. Lappalainen, R. Seppänen, S. Miettinen, Adipose stem cell tissue-engineered construct used to treat large anterior mandibular defect: a case report and review of the clinical application of good manufacturing practice-level adipose stem cells for bone regeneration, J. Oral Maxillofac. Surg. 71 (2013) 938–950, https://doi.org/10.1016/j.joms.2012.11.014.

[79] S. Kotani, Y. Fujita, T. Kitsugi, T. Nakamura, T. Yamamuro, C. Ohtsuki, T. Kokubo, Bone bonding mechanism of beta-tricalcium phosphate, J. Biomed. Mater. Res. 25 (1991) 1303–1315, https://doi.org/10.1002/jbm.820251010.

[80] M. Neo, S. Kotani, Y. Fujita, T. Nakamura, T. Yamamuro, Y. Bando, C. Ohtsuki, T. Kokubo, Differences in ceramic-bone interface between surface-active ceramics and resorbable ceramics: a study by scanning and transmission electron microscopy, J. Biomed. Mater. Res. 26 (1992) 255–267, https://doi.org/10.1002/jbm.820260210.

[81] I.R. Zerbo, A.L.J.J. Bronckers, G. de Lange, E.H. Burger, Localisation of osteogenic and osteoclastic cells in porous β-tricalcium phosphate particles used for human maxillary sinus floor elevation, Biomaterials 26 (2005) 1445–1451, https://doi.org/10.1016/j.biomaterials.2004.05.003.

[82] H. Lu, Z.Y. Ma Y, L. Xiao L, J.W. Zhang Y, Current application of beta-tricalcium phosphate in bone repair and its mechanism to regulate osteogenesis, Front Mater 8 (2021) 1–16, https://doi.org/10.3389/fmats.2021.698915.

[83] Y. Maazouz, I. Rentsch, L. Bin, B. Le Gars Santoni, N. Doebelin, M., in vitro measurement of the chemical changes occurring within β-tricalcium phosphate bone graft substitutes, Acta Biomater. 102 (2020) 440–457, https://doi.org/10.1016/j.actbio.2019.11.035.

[84] L. Liang, P. Rulis, W.Y. Ching, Mechanical properties, electronic structure and bonding of α-and β-tricalcium phosphates with surface characterization, Acta Biomater. 6 (2010) 3763–3771, https://doi.org/10.1016/j.actbio.2010.03.033.

[85] L. Boilet, M. Descamps, E. Rguiti, A. Tricoteaux, J. Lu, F. Petit, V. Lardot, F. Cambier, A. Leriche, Processing and properties of transparent hydroxyapatite and β-tricalcium phosphate obtained by HIP process, Ceram. Int. 39 (2013) 283–288, https://doi.org/10.1016/j.ceramint.2012.06.023.

[86] A. Garcia-Prieto, J.C. Hornez, A. Leriche, P. Pena, C. Baudín, Influence of porosity on the mechanical behaviour of single phase β-TCP ceramics, Ceram. Int. 43 (2017) 6048–6053, https://doi.org/10.1016/j.ceramint.2017.01.146.

[87] S. Nakamura, R. Otsuka, H. Aoki, M. Akao, N. Miura, T. Yamamoto, Thermal expansion of hydroxyapatite-β-tricalcium phosphate ceramics, Thermochim. Acta 165 (1990) 57–72, https://doi.org/10.1016/0040-6031(90)80206-E.

[88] E.D. Case, J.R. Smyth, O. Hunter, Grain-size dependence of microcrack initiation in brittle materials, J. Mater. Sci. 15 (1980) 149–153, https://doi.org/10.1007/BF00552439.

[89] I.H. García-Páez, R. García-Carrodeguas, A.H. De Aza, C. Baudín, P. Pena, Effect of Mg and Si co-substitution on microstructure and strength of tricalcium phosphate ceramics, J. Mech. Behav. Biomed. Mater. 30 (2014) 1–15, https://doi.org/10.1016/j.jmbbm.2013.10.011.

[90] S. Vanhatupa, S. Miettinen, P. Pena, C. Baudín, Diopside-tricalcium phosphate bioactive ceramics for osteogenic differentiation of human adipose stem cells, J. Biomed. Mater. Res. Part B Applied Biomaterials 108 (2020) 819–833, https://doi.org/10.1002/jbm.b.34436.

[91] S. Tkachenko, M. Horynová, M. Casas-Luna, S. Diaz-de-la-Torre, K. Dvorak, L. Celko, J.M. Kaiser, E.B. Montufar, Strength and fracture mechanism of iron reinforced tricalcium phosphate cermet fabricated by spark plasma sintering, J. Mech. Behav. Biomed. Mater. 81 (2018) 16–25, https://doi.org/10.1016/j.jmbbm.2018.02.016.

[92] Y.H. Hsu, I.G. Turner, A.W. Miles, Mechanical properties of three different compositions of calcium phosphate bioceramic following immersion in Ringer's solution and distilled water, J. Mater. Sci. Mater. Med. 20 (2009), 2367–237.

[93] K. Ohura, T. Nakamura, T. Yamamuro, T. Kokubo, Y. Ebisawa, Y. Kotoura, M. Oka, Bone-bonding ability of P2O5 -Free CaO.SiO2 glasses, J. Biomed. Mater. Res. 25 (1991) 357–361, https://doi.org/10.1002/jbm.820250307.

[94] R. García Carrodeguas, P.N. De Aza, Main contributions to bioceramics by salvador de Aza, Bol. Soc. Esp. Cerám. V. 50 (2011) 301–309, https://doi.org/10.3989/cyv.392011.

[95] P.N. De Aza, F. Guitian, S. De Aza, Bioactivity of wollastonite ceramics- in vitro evaluation, Scripta Metall. Mater. 31 (1995) 1001–1005, https://doi.org/10.1016/0956-716X(94)90517-7.

[96] P.N. De Aza, Z.B. Luklinska, M. Anseau, F. Guitian, S. De Aza, Morphological studies of pseudowollastonite for biomedical application, J. Microsc. 182 (1996) 24–31, https://doi.org/10.1111/j.1365-2818.1996.tb04794.x.

[97] P.N. De Aza, Z.B. Luklinska, M.R. Anseau, F. Guitian, S. De Aza, Bioactivity of pseudowollastonite in human saliva, J. Dent. 27 (1999) 107–113, https://doi.org/10.1016/S0300-5712(98)00029-3.

[98] P.N. De Aza, Z.B. Luklinska, A. Martinez, M.R. Anseau, F. Guitian, S. De Aza, Morphological and structural study of pseudowollastonite implants in bone, J. Microsc. 197 (2000) 60–67, https://doi.org/10.1046/j.1365-2818.2000.00647.x.

[99] I. Kotsis, A. Balogh, Synthesis of wollastonite, Ceram. Int. 15 (1989) 79–85, https://doi.org/10.1016/0272-8842(89)90018-7.

[100] L.Z. Zhu, H.Y. Sohn, T.M. Bronson, Flux growth of 2M-wollastonite crystals for the preparation of high aspect ratio particles, Ceram. Int. 40 (2014) 5973–5982, https://doi.org/10.1016/j.ceramint.2013.11.045.

[101] P.N. De Aza, F. Guitian, Phase diagram of wollastonite-tricalcium phosphate, J. Am. Ceram. Soc. 78 (1995) 1653–1656, https://doi.org/10.1111/j.1151-2916.1995.tb08865.x.

[102] L.H. Long, L.D. Chen, S.Q. Bai, J. Chang, K.L. Lin, Preparation of dense β-CaSiO3 ceramic with high mechanical strength and HAp formation ability in simulated body fluid, J. Eur. Ceram. Soc. 26 (2006) 1701–1706, https://doi.org/10.1016/j.jeurceramsoc.2005.03.247.

[103] T. Endo, A. Sugiur, M. Sakamaki, H. Takizwa, M. Shimada, Sintering and mechanical properties of β-wollastonite, J. Mater. Sci. 29 (1994) 1056–1504.

[104] K. Lin, W. Zhai, S. Ni, J. Chang, Y. Zeng, W. Qian, Study of the mechanical property and in vitro biocompatibility of CaSiO3 ceramics, Ceram. Int. 31 (2005) 323–326, https://doi.org/10.1016/j.ceramint.2004.05.023.

[105] H.I. García-Páez, P. Pena, C. Baudin, M.A. Rodríguez, E. Córdoba, A.H. De Aza, Processing and in vitro bioactivity of a β-Ca3(PO4)2–CaMg(SiO3)2 ceramic with the eutectic composition, Bol. Soc. Esp. Ceram. Vidr. 55 (2016) 1–12, https://doi.org/10.1016/j.bsecv.2015.10.004.

[106] S. Nakajima, Y. Harada, Y. Kurihara, T. Wakatsuki, H. Noma, Physicochemical characteristics of new reinforcement ceramic implant, Shikwa Gakuho 89 (1989) (1989) 1709–1717 (English abstract).

[107] S. Nakajima, Experimental studies of healing process on reinforcement ceramic implantation in rabbit mandible, Shikwa Gakuho 90 (1990) 525–553 (English abstract).

[108] Y. Miake, T. Yanagisawa, Y. Yajima, H. Noma, N. Yasui, T. Nonami, High-resolution and analytical electron microscopic studies of new crystals induced by a bioactive ceramic (diopside), J. Dent. Res. 74 (1995) 1756–1763, https://doi.org/10.1177/00220345950740110701.

[109] C. Wu, J. Chang, Degradation, bioactivity, and cytocompatibility of Diopside, Akermanite, and bredigite ceramics, J. Biomed. Mater. Res. Part B: Appl. Biomater. 83B (2007) 153–160, https://doi.org/10.1002/jbm.b.30779.

[110] C. Wu, Y. Ramaswamy, H. Zreiqat, Porous diopside (CaMgSi2O6) scaffold: a promising bioactive material for bone tissue engineering, Acta Biomater. 6 (2010) 2237–2245, https://doi.org/10.1016/j.actbio.2009.12.022.

[111] P.N. De Aza, Z.B. Luklinska, M.R. Anseau, M. Hector, F. Guitián, S. De Aza, Reactivity of a wollastonite-tricalcium phosphate Bioeutectic® ceramic in human parotid saliva, Biomaterials 21 (2000) 1735–1741, https://doi.org/10.1016/S0142-9612(00)00058-2.

[112] T. Sata, Phase relationship in the system 3CaOP2O5–CaO·MgO·2SiO2–SiO2, Bull. Chem. Soc. Jpn. 32 (1959) 105–108.
[113] R. García Carrodeguas, A.H. De Aza, I. García-Páez, S. De Aza, P. Pena, Revisiting the phase-equilibrium diagram of the Ca3(PO4)2–CaMg(SiO3)2 system, J. Am. Ceram. Soc. 93 (2010) 561–569, https://doi.org/10.1111/j.1551-2916.2009.03425.x.
[114] J. Parra, I.H. García Páez, A.H. De Aza, C. Baudin, M.R. Martín, P. Pena, In vitro study of the proliferation and growth of human fetal osteoblasts on Mg and Si co-substituted tricalcium phosphate ceramics, J. Biomed. Mater. Res. PartA 105 (2017) 2266–2275, https://doi.org/10.1002/jbm.a.36093.
[115] M.A. Sainz, P. Pena, S. Serena, A. Caballero, Influence of design on bioactivity of novel CaSiO3–CaMg(SiO3)2 bioceramics: in vitro simulated body fluid test and thermodynamic simulation, Acta Biomater. 6 (2010) 2797–2807, https://doi.org/10.1016/j.actbio.2010.01.003.
[116] A.H. De Aza, P. Velasquez, M.I. Alemany, P. Pena, P.N. De Aza, In situ bone-like apatite formation from a Bioeutectic® ceramic in SBF dynamic flow, J. Am. Ceram. Soc. 90 (4) (2007) 1200–1207, https://doi.org/10.1111/j.1551-2916.2007.01534.x.
[117] E. Meurice, F. Bouchart, J.C. Hornez, A. Leriche, D. Hautcoeur, V. Lardot, F. Cambier, M.H. Fernandes, F. Monteiro, Osteoblastic cells colonization inside beta-TCP macroporous structures obtained by ice-templating, J. Eur. Ceram. Soc. 36 (2016) 2895–2901, https://doi.org/10.1016/j.jeurceramsoc.2015.10.030.
[118] L.J. Gibson, Biomechanics of cellular solids, J. Biomech. 38 (2005) 377–399, https://doi.org/10.1016/j.jbiomech.2004.09.027.
[119] Microstructure and Fracture Behaviour of Porous β-tricalcium Phosphate/diopside Composite Scaffolds, to Be Published.